A Study Into Pyrolysis Of Biomass In Combination With CO2 Reforming And Its Subsequent Effect On C/N-cycles

by

Andreas Larsson

June 2024

Department of Sustainable Energy
Department of Chemical Engineering
Lund University

Supervisor: **Hesameddin Fatehi, Lund University**
Lund University Examiner: **Ola Wallberg, Lund University**

Postal address
Box 124
SE-221 00 Lund, Sweden
Web address
http://www.ple.lth.se

Visiting address
Kemicentrum
Naturvetarvägen 14
223 62 Lund, Sweden

Telephone
+46 46-222 82
+46 46-222 00

Acknowledgements

I would like to start off by thanking my supervisor, Hesameddin Fatehi, for giving me the opportunity to work on such an interesting project. Your advice and helpful feedback throughout the thesis made everything work out smoothly. Also, I really enjoyed our scientific discussion on the different topics. I would also like to thank my examiner Ola Wallberg for examining my thesis and for the several helpful pieces of advice when I was stuck with the simulations. Lastly, I would like to thank my friends, family and especially my girlfriend for your support during this thesis.

Populärvetenskaplig sammanfattning

Biomassa och Teknologi för en Hållbar Framtid

Genom pyrolys omvandlas biomassa till biokol, bioolja och biogas, vilket minskar beroendet av fossila bränslen och ger hållbara kemikalier, bränslen och energi. Detta motverkar global uppvärmning samtidigt som biokolet minskar behovet av gödningsmedel, vilket motverkar övergödning av våra sjöar och hav.

Sedan den industriella revolutionen har människan använt kol och olja till allt från energi, tillverkning av plaster och läkemedel, samt för att värma våra hem och driva våra bilar. Denna användning har släppt ut stora mängder koldioxid (CO_2) i atmosfären, vilket i sin tur lett till den globala uppvärmningen. Samtidigt har avverkning av skogar, som annars skulle absorbera CO_2 genom fotosyntesen, ytterligare rubbat det naturliga kolkretsloppet. Dessutom har överanvändning av kvävebaserade gödningsmedel rubbat kvävekretsloppet och orsakat övergödning i våra sjöar och hav, vilket har påverkat många ekosystem. För att återställa balansen i dessa kretslopp på vår planet måste vi hitta nya teknologier för att hantera dessa problem.

En föreslagen lösning är pyrolys av trä, stjälkar och matavfall. Pyrolys innebär att organiskt material upphettas till temperaturer ofta runt 300 upp till 1300 grader Celsius utan av syre. Detta bryter ner biomassan till biokol, bioolja och biogas istället för koldioxid och vatten som vid förbränning. Dessa produkter har flera användningsområden: biokolet kan modifieras och användas som gödningsmedel, biooljan kan genom CO_2-reformering omvandlas till syngas för tillverkning av kemikalier och bränslen, och biogasen kan förbrännas för att ge energi till resten av processen. Processen är inte bara koldioxidneutral utan även kol negativ, vilket innebär att den tar bort koldioxid från atmosfären och binder den i biokol och syngasprodukter. Detta kan hjälpa till att återställa ett naturligt kol- och kvävekretslopp och motverka global uppvärmning och övergödning. Målet med det här exjobbet var att utvärdera processens påverkan på kol- och kvävecykler, analysera energi- och kolflöden genom processen samt optimera driftsförhållanden för att maximera produktionen av syntesgas.

För att kunna svara på målet med exjobbet, genomfördes simuleringar i Aspen Plus V.14. Detta visade att processen kan fånga upp till 70% av kolet som stoppas in i processen och därmed minskar mängden koldioxid i atmosfären. Vilket betyder att processen kommer att hjälpa världen att återgå till ett mer naturligt kol kretslopp och minska global uppvärmning. Simulerings resultaten visade också att anpassa driftförhållanden för att maximera syngas produktion är viktigt. En litteraturstudie av biokolet som gödningsmedel visade att det kan minska behovet av traditionella kvävebaserade gödningsmedel. Detta genom att förbättra växternas kväveupptag och minska kväveförluster till sjöar och hav. Vilket i sin tur leder till att motverka övergödning och återställa ett naturligt kvävekretslopp.

Abstract

Anthropogenic activities, such as using fossil fuels for energy production, synthesizing carbon-based products, and employing nitrogen fertilizers to meet the ever-growing food demand, have drastically disrupted the planet's carbon and nitrogen cycles. These activities effectively lead to global warming, eutrophication, and NOx production. Hence, the world is in need of coming up with new sustainable technological advancements to meet the demands of fuel synthesis, carbon-based material manufacturing and food production without impacting the world's natural carbon and nitrogen cycles. One proposed solution is to utilize pyrolysis of sustainable biomass to produce biochar, bio-oil, and pyrolysis gas. The bio-oil obtained from this process can be used in a CO2 reforming step, effectively converting it into syngas with a suitable H2/CO ratio for chemical synthesis or fuel production. The produced biochar can, through a CO2 activation step and adsorption of nitrogen, be used as a fertilizer. Lastly, combustion of the produced pyrolysis gas generates energy for the other processes in the system.

In this master thesis, the aim was to evaluate the impact of the process on carbon and nitrogen cycles, analyze energy and carbon flows throughout the process, and optimize operational conditions to maximize syngas production. In addition, the study also addressed several research questions. These included investigating whether the process necessitates the introduction of external sustainable energy, and assessing the overall environmental impact of the process. To answer these research questions and overall aim, a model of the process was made in Aspen Plus V.14 in combination with a literature study on the biochars effect on the nitrogen cycle.

The results indicate that up to 70% of the carbon going into the process can be successfully sequestered through the optimization of pyrolysis for bio-oil production and subsequently of syngas yield in CO2 reforming. The study also saw that using a combined steam and CO2 reforming process could be beneficial for syngas yield and sequestration of carbon. Another conclusion was that sufficient energy was generated in the Mild combustion step for the other processes within the system, effectively eliminating the need for the introduction of renewable resources. Overall, the process will diminish the anthropogenic impact on the C-cycle by capturing CO2 from the atmosphere and sequestering it into the soil through the biochar and by processing the syngas into carbon-based products. The total sequestered amount will highly depend on the subsequent use and products of the syngas. For the system it was seen that mainly the produced biochar will have an impact on the N-cycle, effectively reducing the needed amount of added nitrogen fertilizer to the soil by reducing ammonia volatilization and increasing the nitrogen uptake by the plants.

Table of contents

1. Introduction..... 1
1.1 Aim and Research Questions..... 2
2. Background..... 3
2.1 General Process Description..... 3
2.2 Sustainable Biomass..... 4
2.3 Pyrolysis Process..... 4
2.3.1 Pyrolysis..... 4
2.3.2 Biochar..... 5
2.3.2.1 Biochar As Fertilizer..... 6
2.3.3 Bio-oil..... 7
2.3.3.1 Bio-oil Application..... 7
2.3.4 Pyrolytic Gas..... 7
2.4 Mild Combustion..... 8
2.5 NOx Production..... 8
2.6 CO2 Reforming..... 9
2.7 CO2 Activation Of Biochar..... 10
2.8 Carbon Cycle..... 10
2.9 Nitrogen Cycle..... 11
3. Method..... 12
3.1 Aspen Plus..... 12
3.1.1 Aspen Plus Process Flowsheet..... 13
3.1.2 Model Components..... 15
3.1.3 Thermodynamic Framework..... 17
3.1.4 The Entered Properties..... 17
3.1.5 Calculations..... 18
4.Results And Discussion..... 19
4.1 Pyrolysis Verification And Optimization..... 19
4.1.1 Pyrolysis Optimization..... 22
4.2 Mild Combustion Verification..... 24
4.3 CO2 Reforming Verification..... 26
4.4 Configuration Evaluation..... 28
4.4.1 Configuration 1..... 28
4.4.2 Process Optimization..... 31
4.4.3 Configuration 2..... 34
4.4.4 Configuration 3..... 35
4.5 Process Impact On The C-cycle..... 38
4.6 Process Impact On The N-cycle..... 39

4.7 Sustainability Of The Process.....40
5. Conclusion.....42
6. Future work.....43
7. Reference list.....44
Appendix A.....50
Appendix B.....50
Appendix C.....51

1. Introduction

The combustion of fossil fuels as well as its use in chemical synthesis, and other anthropogenic activities such as heavy dependency on nitrogen fertilizer have dramatically increased global warming and at the same time distorted the C/N-compound cycle of the planet. To simply stop the use of fossil fuels and fertilizers is not possible due to their importance in today's society. Fossil fuels are vital for meeting global energy demands, serving as fuel for transportation, and deeply integrated in the global economy. Furthermore, fossil fuels are essential for the production of essential chemicals, pharmaceuticals, and other carbon-based materials used in everyday life. Additionally, the world requires more fertilizer to meet the increasing food demands for the growing global population, while also facing the challenge of managing limited farming areas, avoiding deforestation, and preserving natural habitats for wildlife. This leaves the world in a drastic need to search for new technological advancements combined with the use of sustainable resources to create a sustainable C/N cycle while simultaneously meeting the essential product demands of everyday life.

One proposed solution to face this problem is the MINICOR project by the European Union. The proposed project utilizes pyrolysis of sustainable biomass in combination with CO2 reforming of the subsequently produced bio-oil. This will convert the bio-oil into syngas with a suitable H2/CO ratio for chemical synthesis or fuel production. Additionally, syngas is a substitute for fossil fuels in high-temperature processes, which are often inefficient to power with electricity generated from renewable resources such as wind or solar. The syngas can be directly introduced into our existing fossil fuel infrastructure, reducing the necessity for high initial investment costs needed for rebuilding the current fossil fuel-based plants. Furthermore, the biochar produced in the pyrolysis, can with an activation step of CO2 be used to absorb nitrogen, making it suitable as a fertilizer. The last product of the pyrolysis, the pyrolysis gas can be combusted in a Mild combustion to generate heat for the rest of the system. Through analysis and optimizing the pyrolysis and CO2 reforming processes, the process helps mitigate the environmental impact of anthropogenic activities and contributes to the creation of a sustainable C/N-cycle.

1.1 Aim and Research Questions

This thesis aims to evaluate the impact of the process on carbon and nitrogen cycles, analyze energy and carbon flows throughout the process, and optimize operational conditions to maximize syngas production.

The following research questions were formulated and answered in this study.

- How does the optimization of different reactor conditions in the pyrolysis and CO2 reforming affect the overall C/N balance?
- How does the utilization of nitrogen capture through activated biochar affect the C/N cycle as well as the biochar's contribution to soil carbonization and nitrification?
- Is external renewable energy needed to be introduced into the system?
- How is the C/N cycle affected through every step in the process?
- How can the C/N management improve the environment?

2. Background

2.1 General Process Description

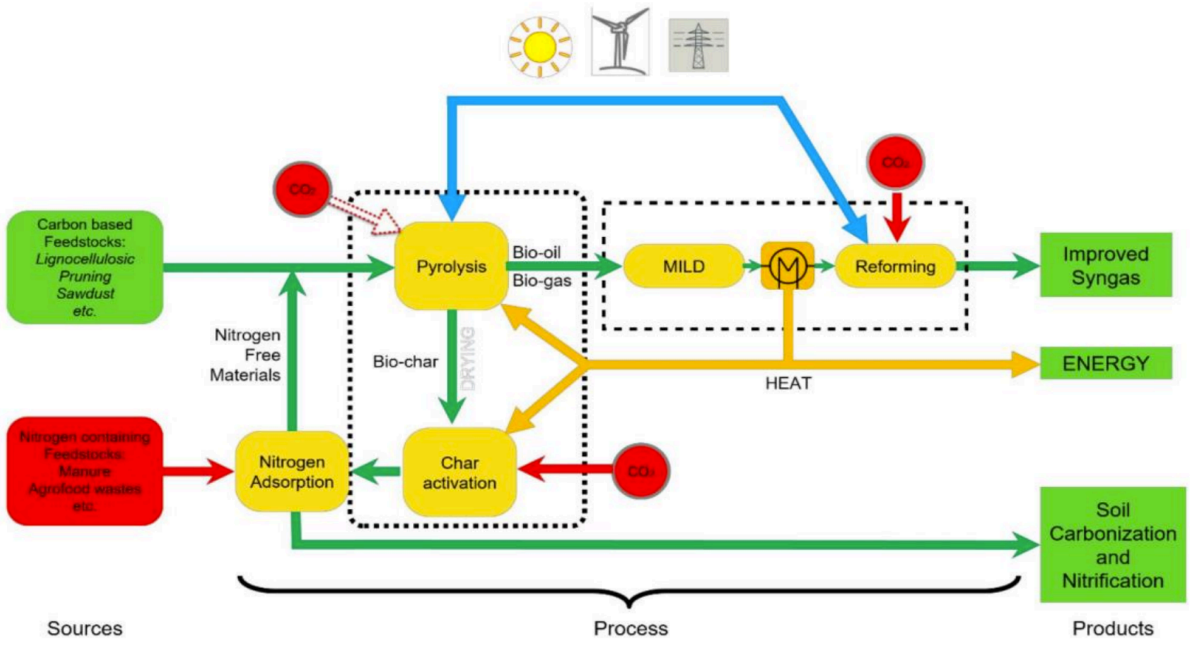

Figure 1: General description of the process.

Figure 1 describes the proposed process to maximize the utilization of the biomass to reduce CO2 emissions while creating a sustainable C/N cycle. The process starts with carbon-based feedstock being fed into the pyrolysis reactor. From this, three products are produced: bio-oil, bio-gas/pyrolysis gas, and biochar. The amount and composition of these products highly depends on the feedstock and pyrolysis conditions. The produced pyrolysis gas is then combusted under Mild conditions generating energy that can be utilized in the other parts of the process. Mild combustion, compared to classical combustion, reduces the amount of produced air pollutants. The bio-oil product is then reformed with carbon dioxide generated during the Mild combustion to produce syngas. Lastly, the biochar can also be activated with carbon dioxide generated from the Mild combustion, this activation makes it possible for the biochar to adsorb nitrogen. The activated biochar can then be used as a fertilizer. The valorization of the produced carbon products and the subsequent carbon dioxide generated by Mild combustion make this process carbon negative, thus reducing the amount of CO2 in the atmosphere. There is also the possibility of adding sustainably produced energy into the process if the energy created from the Mild combustion is not enough for the whole process. In the coming section all of the processes, feedstock selection and products will be discussed in depth.

2.2 Sustainable Biomass

For this process, sustainable biomass is going to be utilized as a replacement for fossil fuels. Biomass is an organic material from living organisms, such as plants, microorganisms, and animals, as well as residues and byproducts produced from living organisms. Even though biomass is a renewable resource it is important to note that renewable does not mean sustainable. Several requirements have to be met in order for the biomass to count as sustainable. The production of sustainable biomass needs to have a low environmental impact. This includes several factors such as biodiversity preservation, soil conservation, water use, and land use. The land use is an important factor because it leads to conflicts between biomass produced for energy and that produced as food. It is also important that the processing of the biomass such as transportation and harvesting is sustainable as well. Lastly, for sustainable biomass the social aspects are also important, it should avoid negative impact on local communities and reduce poverty (Wiebren De Jong and Ommen, 2015).

Being sustainable is not the only demand on biomass for the feedstock selection; other important factors include its effect on the product yields as well as generating favorable qualities of those products. Such as being non-toxic and contributing to CO2 sequestration. The importance of these factors will be mentioned in the upcoming section on the products of the process.

2.3 Pyrolysis Process

2.3.1 Pyrolysis

Pyrolysis is a thermochemical process that involves subjecting biomass to temperatures around 200 °C up to 700 °C in the absence of oxygen. The biomass decomposes at these temperatures into biochar, bio-oil also called pyrolytic oil, and pyrolysis gas. These three main products have different uses and can be produced in different amounts based on operating conditions. Pyrolysis can be divided into three types, slow pyrolysis, fast pyrolysis, and flash pyrolysis. Slow pyrolysis operates at low temperatures around 200-350 °C and has long residence times; this type of pyrolysis favors biochar production. Fast pyrolysis is conducted at higher temperatures around 450-550°C. This temperature increase and a more rapid heating rate in combination with shorter residence time favors bio-oil production (Wiebren De Jong and Ommen, 2015). Flash pyrolysis involves an even higher temperature of around 900-1300 degrees and generally lower residence time than fast pyrolysis. Flash pyrolysis is favorable for maximizing pyrolysis gas yield (Pahnila et al., 2023), (Li et al., 2013).

The choice of the reactor for pyrolysis can affect the heat transfer rate and product composition. Traditional kilns in different forms are low-cost reactors widely used for the production of biochar. However, these reactors operate slowly, struggle with heat loss, and lack mechanisms to handle the produced pyrolysis gas, which is both toxic and leads to increased global warming. More advanced kilns such as the Adam retort kiln solves this issue by efficiently capturing and utilizing the pyrolysis gas, thereby reducing emissions and improving overall energy efficiency (Cornelissen et al., 2016). For a fast pyrolysis favoring bio-oil yield, there are several different reactors, many of which are based on mixing biomass particles with a preheated heat carrier, such as sand. This technique is commonly found in fluidized bed reactors. Fluidized bed reactors suspend biomass particles in heated inert materials such as

sand using a fluidizing gas (IEA Bioenergy, n.d.). According to Kaminsky (2021) fluidized bed reactors are a good choice for bio-oil production via fast pyrolysis. This is because of their efficient heat transfer, uniform temperature distribution and controlled residence time. Other reactors such as ablative pyrolysis reactors rely on mechanical force that pressesses the biomass on a heated surface. There are also many others like pyrolysis reactors such as microwave pyrolysis reactor, cyclone reactor and rotating cone reactor. The choice of reactor highly depends on wanted product and quality as well as possible scale up possibility (IEA Bioenergy, n.d.).

The choice on how to heat up the reactor is also important, there are several different forms of heating alternatives. As mentioned before, hot sand and gas heat carriers, such as nitrogen, can be used to heat up the biomass in the reactor; this is called direct heating. The heat used for the direct heat exchange can be achieved by burning pyrolysis gas or the produced biochar. In contrast, indirect heating methods include heating the reactor wall or built-in tubes or plates, here as well there is the possibility to utilize the pyrolysis gas. The produced hot exhaust gasses can be used directly to heat up the reactor wall or plates, or its energy can be transferred in a heat exchanger to heat the reactor. Another alternative is using an electrical pyrolysis reactor, which can be heated using electricity from renewable resources (IEA Bioenergy, n.d.).

2.3.2 Biochar

Biochar is a solid residue left after the more volatile components have left the biomass. This biochar, mainly composed of carbon, can play an important role as a fertilizer or for removing heavy metals from water or soil. The composition of biochar can be divided into organic compounds and inorganic compounds. Carbon, oxygen, hydrogen, sulfur and nitrogen are most common in organic matter, while mineral elements in the biochar ash include phosphorus, calcium, aluminum, magnesium, silica, potassium and sodium. Biochar has various functional groups such as hydroxyl, epoxy, carbonyl, carboxyl, ether and ester. The carboxyl and phenolic carbon groups tend to possess a higher cation exchange capacity (CEC), which means it improves the biochar capability to absorb nutrients (Jindo et al., 2020).

The biochar properties are highly dependent on the chosen feedstock, temperature and possible pretreatment of the biomass. Jindo et al (2020) also mentions how lignocellulosic biomass tends to produce a higher amount of aromatic C groups as well as graphite around 500 °C and how this causes the hydrophobicity of the biomass to increase. This leads to an increase in the biomass capability to absorb nutrients. The biochar reaches its maximum yield at lower temperatures (200–350C), often by using larger lignocellulosic particles as feedstock. This type of pyrolysis is generally known as slow pyrolysis or carbonization (Wiebren De Jong and Ommen, 2015). From lignocellulosic biomass it has been shown that lignin leads to higher amounts of produced biochar compared to cellulose and hemicellulose. Furthermore, the biochar yield drastically decreases with increased temperature meanwhile bio-oil and pyrolysis gas increases. However, it is worth noting that even at high pyrolization temperatures of around 800 °C 56% wt of lignin is converted into biochar (Devi and Saroha, 2014).

The biochar must not contain any toxic compounds since it is going to become a fertilizer. Therefore the biomass feedstock should generally avoid heavy metals as they could be leaching from the biochar as

shown (Devi and Saroha, 2014). This limits the possible recycling of old treated wood waste that had been impregnated with heavy metals such as CCA (copper, chromium and arsenic). However, when old furniture is coated with urea-formaldehyde resin, it was shown that the amount of nitrogen in the biochar increased, which is only beneficial for its use as a fertilizer (Liu et al., 2023).

Experimental observations by Bednik, Agnieszka Medyńska-Juraszek and Irmina Ćwieląg-Piasecka, 2022) suggest that lignocellulosic biomass from wood, straw, grass, or seed husks exhibit greater resistance to degradation in the environment compared to food wastes. Having a greater resistance to degradation makes it more suitable for long term carbon sequestration.

2.3.2.1 Biochar As Fertilizer

To be an effective fertilizer the biochar needs to improve the nitrogen, phosphorus, and potassium concentrations in the soil as they are the most important growth nutrients for plants. The amount of these components in the biochar can depend on the feedstock and pyrolysis conditions. The nitrogen content in the biochar is feedstock and temperature dependent, the amount is generally low for biochar (Jindo et al., 2020). However, Jedynak and Charmas (2021) showed that a CO2 activation of the biochar could lead to increased ammonium adsorption compared to non-activated biochar. Although, it should be mentioned that chemically activated biochar showed even better results, compared to the CO2 activated one. The low amount of nitrogen in the biochar means that the biochar is going to have to be mixed with other nitrogen fertilizer, the effect of which is going to be more discussed in section 4.6. Another study on the activation of biochar suggests that biochar activation in combination with the premixing of mineral fertilizer showed reduced N and P leaching (Brtnicky et al., 2023).

According to Jindo et al (2020), biochar can affect phosphorus levels both directly and indirectly by adding extra phosphorus into the soil as well as shifting microbial community composition and changing soil pH. Phosphorus is naturally occurring in all biomass although it is more common in crop residue and manure than forest residue. Higher temperatures favor higher quantities of inorganic phosphorus (orthophosphate) in the biochar compared to lower-temperature pyrolysis which favors organic phosphorus (pyrophosphate). Plants more favorably take up inorganic phosphorus than organic phosphorus. Overall biochar helps the soil by adding extra phosphorus already existing in the biochar. The amount of phosphorus is also indirectly improved by biochar's ability to enhance microbial activity thus increasing the decomposition of organic matter and enzyme release, subsequently increasing the amount of soluble phosphorus for the plant to take up. However, it needs to be mentioned that the reverse effect has been seen in low-concentration phosphorus acidic soils where sorption of the phosphorus by the biochar in combination with improved microbial activity reduced the available phosphorus for the plants. The biochar complexity with pH levels in the soil is added to by the fact that biochar can also help with reducing phosphorus fixation in acidic soils. Since the biochar is basic it highers the pH of the soil effectively making some insoluble Al- or Fe-P minerals soluble when pH reaches above 7 (Jindo et al., 2020).

Biochar often has high quantities of potassium, however, the amount of water-soluble is dependent on the temperature used for the pyrolysis. The water-soluble potassium amount seems to increase until around 600°C with a clear drop at 700 °C. The insoluble part of the potassium in the biochar dissolves very

slowly over time. Some reports mentions that the use of biochar can lead to increased K-leaching. However, overall the biochar nonetheless leads to an increase in potassium amount in the soil which is good for the plant-growth. (Jindo et al., 2020) Using biochar as a fertilizer has also been shown in a meta-analysis by Han et al (2023) to increase nitrogen efficiency, water efficacy, and increase overall crop yield.

2.3.3 Bio-oil

Bio-oil or pyrolysis oil is a product that is produced from biomass as it goes through pyrolysis. The composition and yield for the bio-oil is highly dependent on several factors such as pretreatment of the biomass, temperature of the pyrolysis and feedstock. Bio-oil consists of phenols, acids, aldehydes, ketones, furans, alcohols, esters and relatively high amounts of water. The water causes the bio-oil to have a comparatively low heating value compared to petroleum oil and the acids in the bio-oil causes it to be corrosive. Nevertheless, bio-oil has a higher volumetric energy density than biomass making it more effective for transportation compared to the bulky biomass and its better from an environmental point of view than petroleum (Lyu, Wu and Zhang, 2015) (Wiebren De Jong and Ommen, 2015).

Maximizing the bio-oil yield by the selection of biomass feedstock is important as the bio-oil is later used to produce the main product of the process, the syngas. According to a study done by Chen et al (2022) on pyrolysis in lignocellulosic biomass, it was concluded that cellulose produces a maximum value of 67.5% wt, for hemicellulose 55.3% wt at 450 °C and lastly lignin produces bio-oil yield of at 28.7% wt at 550 °C. Since the standard composition of lignocellulose biomass cellulose (35%–50%), hemicellulose (20%–35%), and lignin (10%–25%), a suitable biomass should therefore be rich in cellulose and hemicellulose compared to lignin (Chen et al., 2022).

2.3.3.1 Bio-oil Application

The bio-oil can be used directly for heating or power generation. Even though liquefied biomass (bio-oil) can more or less be directly introduced into our already-built infrastructure for petroleum, it has some problems. This is due to corrosiveness and that the low heating value leads to ignition problems as well as a much larger amount of bio-oil needed compared to oil from fossil fuels. However, it is suggested that it can be used as ship fuel with a few modifications. Another use for bio-oil is for the production of chemicals since it already consists of several chemicals such as acetic acid, acetol, glucose (levoglucosan), and phenol. These compounds can both be directly extracted from the bio-oil or its composition could be changed with further processing. For the use of bio-oil as a chemical feedstock it is very important to improve selectivity of the targeted chemicals through optimizing the pyrolysis conditions and biomass selection. Lastly through gasification, bio-oil can be transformed into syngas better suited for the already built chemical industries for petroleum oil(Wiebren De Jong and Ommen, 2015).

2.3.4 Pyrolytic Gas

From lignocellulosic biomass, the most common products in pyrolysis gas are CO2, CO, H2, and CH4, which accounted for more than 95 vol.% of the total generated pyrolysis gas in an experiment by Chen et

al (2022). The gas yield increases with increasing temperature of the pyrolysis process, in turn, the energy of the gas increases. The volumetric energy density of pyrolytic gas is around 50% of natural gas. However, pyrolytic gas can be directly used for combustion and is better for the environment than natural gas. (Chen et al., 2022).

2.4 Mild Combustion

Mild combustion or moderate intense low-oxygen dilution is a combustion technique implemented to reduce emissions of NOx and other pollutants. Mild combustion is a subset of High Temperature Air Combustion (HiTAC) where the air mixes with the fuel at such a high temperature that the fuel reaches auto-ignition. Mild combustion is based on the same technique but does not have to use stoichiometric air to react with the fuel. While there are several proposed definitions of Mild combustion Cavaliere and de Joannon (2004) define it as "A combustion process is named Mild when the inlet temperature of the reactant mixture is higher than mixture self-ignition temperature whereas the maximum allowable temperature increase concerning inlet temperature during combustion is lower than mixture self-ignition temperature (in Kelvin)." Which can be translated to for simplicity $(T_{in} > T_{si})$ and $(\Delta T < T_{si})$ for the combustion to fall within the Mild combustion definition. It is important to note that different self-ignition temperatures may be obtained for different fuel/oxygen and diluent compositions which needs to be taken into account. The temperature control of the Mild combustion is controlled by changing the input ratio between the fuel/oxygen and nitrogen. A lower amount of oxygen leads to an excess amount of fuel which in turn leads to a lower amount of released exothermic energy and therefore lower combustion temperatures (Cavaliere and de Joannon, 2004). This is not favorable though as it leads to unburnt pyrolysis gases and more wasted energy. It is better to increase the nitrogen ratio leading to more of the combustion energy going to heating up the nitrogen.

2.5 NOx Production

NOx can naturally be produced through photochemical reactions, reacting nitrogen and oxygen under sunlight and from the high temperatures caused by lightning strikes. Most NOx is produced through combustion from three mechanisms: thermal NOx, prompt NOx, and fuel NOx. Thermal NOx is produced at high-temperature combustion where nitrogen from the air reacts with oxygen, this mechanism is the leading cause of NOx production. Prompt NOx is mainly produced through the radicals formed from the fuel reacting with atmospheric nitrogen, leading to nitrogen radicals and finally NOx production. Fuel NOx comes from the nitrogen already present in the fuel reacting with oxygen during combustion and is therefore limited to the amount of nitrogen present in the fuel. The increased NOx concentration affects the environment through the transformation of nitrogen gas into nitric acid in the atmosphere, which can lead to acidic rain, impacting soil pH. However, the main problem with NOx produced from vehicles and other combustion processes is that it can lead to ground-produced ozone and smog, which in turn irritates the airways and can generate decreased lung function. Mitigating NOx production is therefore important for both human health and the environment. (utslappisiffror.naturvardsverket.se, n.d),(DeLacy, 2018).

2.6 CO2 Reforming

CO2 reforming, also known as dry reforming, is a technology developed to reduce CO2 emissions. By reacting CO2 with other carbon-containing species like methane or bio-oil with a catalyst or at high temperatures the CO2 and the bio-oil get converted into syngas. In comparison with the more developed steam reforming technology the produced syngas is characterized by its low H2/CO ratio making it ideal for chemical synthesis like acetic acid, ethanol, oxo-synthesis, and dimethyl ether (DME). CO2 reforming of bio-oil is a very complex process, where several possible reactions can take place, including thermal degradation of the bio-oil, reaction between CO2 and the bio-oil, or if water is present steam reforming. Steam reforming is another way commonly used for hydrogen or syngas production but it produces a syngas with a higher H2/CO ratio. The complexity reactions present during CO2 reforming of bio-oil can be seen in Table 1. The water gas shift (WGS) is an important reaction, since the equilibrium and composition can be shifted through temperature change or concentration. In Landa et al (2023) several experiments of dry reforming of bio-oil were conducted and there were some interesting conclusions. It was concluded that a CO2/C (CO2 to carbon in bio-oil) ratio of 1:1 was deemed optimal and that there was a CO2 conversion of around 24%. However, it should be mentioned Landa et al (2023) used a catalyst for their CO2 reforming something that is not going to be used in the process studied in this thesis. This is done in order to save precious noble metals that the catalyst often consists of. Because of this a higher temperature of around 800-900 degree celcius is going to be used. Similar results to Landa et al (2023) were confirmed by an experiment by Fu et al (2016).

Table 1: The proposed reactions in a steam/dry reforming by (Landa et al., 2023c).

Reaction Number	Name	Chemical Reaction
1	Global SR of bio-oil	$C_nH_mO_k + (2n-k)H_2O \rightarrow nCO_2 + (2n + m/2 - k)H_2$
2	SR of bio-oil	$C_nH_mO_k + (n-k)H_2O \rightarrow nCO + (n + m/2 - k)H_2$
3	Water-Gas-Shift (WGS)	$CO + H_2O \leftrightarrow CO_2 + H_2$
4	DR of bio-oil	$C_nH_mO_k + xCO_2 \rightarrow (n+x)CO + (m/2 - x)H_2 + (x+k)H_2O$
5	Oxygenates cracking (coke)	$C_nH_mO_k \rightarrow C_xH_yOz$ + gas (CO, CO_2, CH_4, C_aH_b, H_2) + C (coke)
6	SR of CH_4	$CH_4 + H_2O \leftrightarrow CO + 3H_2$
7	DR of CH_4	$CH_4 + CO_2 \leftrightarrow 2CO + 2H_2$
8	SR of light hydrocarbons	$C_aH\_b + aH_2O \rightarrow aCO + (a + b/2)H_2$
9	Interconversion of oxygenates	$C_nH_mO_k \rightarrow C_xH_yOz$
10	CH_4 decomposition	$CH_4 \rightarrow 2H_2 + C$
11	Boudouard reaction	$2CO \leftrightarrow C + CO_2$
12	Carbon (coke) gasification	$C + H_2O \rightarrow CO + H_2$

2.7 CO2 Activation Of Biochar

Biochar activation using CO2 was proposed for this process in order to increase the biochar's adsorption capability of nitrogen, and subsequently improve the biochar's use as a fertilizer. The CO2 activation process involves heating biochar to high temperatures of 900°C and adding CO2. The reaction between CO2 and the carbon in the biochar produces carbon monoxide and creates a highly porous structure with increased surface area within the biochar. According to the results by Franciski et al (2018), this significantly increased the adsorption capability of biochar.

However, one thing that needs to be taken into account is that the CO2 activation leads to burn-off. Burn-off refers to the loss of carbon content from the biochar during activation. While some carbon has to react with the CO2 in order to create the desired porous structure, excessive burn-off can reduce the overall yield of activated biochar. Franciski et al (2018) experienced over 22% burn-off in their experiments.

2.8 Carbon Cycle

The carbon cycle is a complex fundamental process that regulates the flow of several different forms of carbon throughout various Earth systems. It involves the transfer of carbon between the oceans, atmosphere, land, and living organisms. During photosynthesis, carbon dioxide is absorbed from the atmosphere and converted into organic carbon by plants. This organic carbon is then decomposed or consumed by animals, releasing carbon dioxide back into the atmosphere through respiration. While carbon dioxide emissions can occur naturally through processes like respiration, photosynthesis, volcanic eruptions, or wildfires, human activities have significantly disrupted the natural carbon cycle. These disruptions include the combustion of stored fossil fuels, which releases carbon dioxide previously kept in natural carbon sinks in the ground. Deforestation is also a problem, which reduces the amount of carbon dioxide absorbed by photosynthesis. The disruption of the carbon cycle has led to increased carbon dioxide levels in the atmosphere, contributing to globally rising temperatures. The ocean has historically acted as an effective carbon sink, slowing down global warming. However, this has led to ocean acidification as a consequence effectively hurting the ecosystems in the ocean (Riebeek, 2011).

Having a comprehensive understanding of the natural carbon cycle is vital. Transitioning to sustainable resources for energy production is crucial in mitigating global warming. Using the combined process of sustainable biomass pyrolysis, with carbon dioxide reforming of the proceed bio-oil and usage of the biochar as a fertilizer makes this system carbon negative. Effectively producing useful by-products while reducing global warming and maintaining a natural carbon cycle.

2.9 Nitrogen Cycle

The nitrogen cycle is important for the movement of nitrogen throughout soil, atmosphere, and water bodies. Nitrogen is an essential element for DNA and protein as it is vital for all living organisms on earth. There are a number of key processes in the nitrogen cycle such as nitrogen fixation, nitrification, denitrification, and ammonification. Nitrogen fixation is done by bacteria either living on their own or in symbiotic relationships with plants, this effectively converts nitrogen gas in the atmosphere into ammonia or ammonium ions which the plant can then use. The animals then obtain their nitrogen from eating the

plants or other animals. The plants or animals can also be decomposed which breaks down the organic nitrogen into ammonia which goes back into the soil, a process known as ammonification. Denitrifying bacteria then closes the circle by transforming the nitrate into nitrogen gas. Human activities have changed the nitrogen cycle, the population increase has also caused an increasing need for food production. This in turn has created a larger need for nitrogen fertilizer, disrupting the natural nitrogen cycle in the soil and causing runoff into rivers and oceans. This leads to eutrophication in the river oceans affecting the entire ecosystem. Another human impact on the nitrogen cycle is through combustion producing nitric oxide and nitrogen dioxide also known as NOx gases. (Encyclopedia Britannica, 2018)

3. Method

This thesis combines process simulation in Aspen Plus with a comprehensive literature study to answer the research questions and the overall aim. The first step was a literature review of relevant research on the four primary processes: Pyrolysis, Mild combustion, CO2 reforming, and bio-char activation with carbon dioxide. Relevant data on these processes, such as feedstock selection, operating conditions, and expected product yield and composition, were taken from existing scientific literature. The next step was to start the process simulations, carried out in Aspen Plus V.14 for the Pyrolysis, Mild combustion, and CO2 Reforming. Various modeling options within Aspen Plus, including reactor selection and accurate biomass representation, were evaluated in order to get an accurate process simulation. This allowed for the examination of how different operating conditions influence product yields, as well as syngas production and composition.

The modeled processes were then validated against the relevant research data from the literary study. Following validation, process optimization was conducted to maximize bio-oil yield. For the overall process results a material balance study was then conducted, to track the carbon flow and transformation throughout the system, offering insights into carbon sequestration potential. Aspen Plus also provided the possibility to analyze energy flow throughout the system and the different options for utilizing the produced energy from the Mild combustion into the other processes. Different configurations were evaluated against each other looking at the differences in carbon and energy flow, potential carbon sequestration of the process and syngas yeild. The nitrogen capture and utilization were only explored through literary sources and not simulated in Aspen Plus. The combined insights from literature studies and process simulations provided a comprehensive understanding of the process's impact on the C/N-cycle, energy efficiency and environmental impact.

3.1 Aspen Plus

This section includes a detailed description of the modeling conducted in Aspen Plus, which included entered properties for the biomass components, choice of reactor, and usage of kinetics for the reactions. Aspen Plus uses a graphical interface that can create process flow diagrams, specify equipment, define process conditions, and simulate the behavior of chemical processes under different scenarios. It is also effective for comprehensive thermodynamic calculations and mass and energy balance calculations which is primarily what is evaluated in this thesis. Even though Aspen Plus was originally designed as a tool for the petrol industry which means the primary design was for liquid and gases and not for solid biomass components. There have been recent attempts to model the biomass decomposition with Aspen Plus as can be seen in (Peters et al., 2017).

Aspen Plus also allows for the usage of extensions like Excel to interactively use Excel for different calculations which are then added into Aspen Plus like in the work of Peters et al (2017). Another possible extension is using Aspen plus custom modeler (ACM). Utilizing ACM allows for adding additional mass and energy transfer between different components as well as momentum transfer as used

in the work by (Humbird et al., 2017),(Caudle, Gorensek and Chen, 2019). In this thesis work, neither the Excel extension nor the ACM were used.

3.1.1 Aspen Plus Process Flowsheet

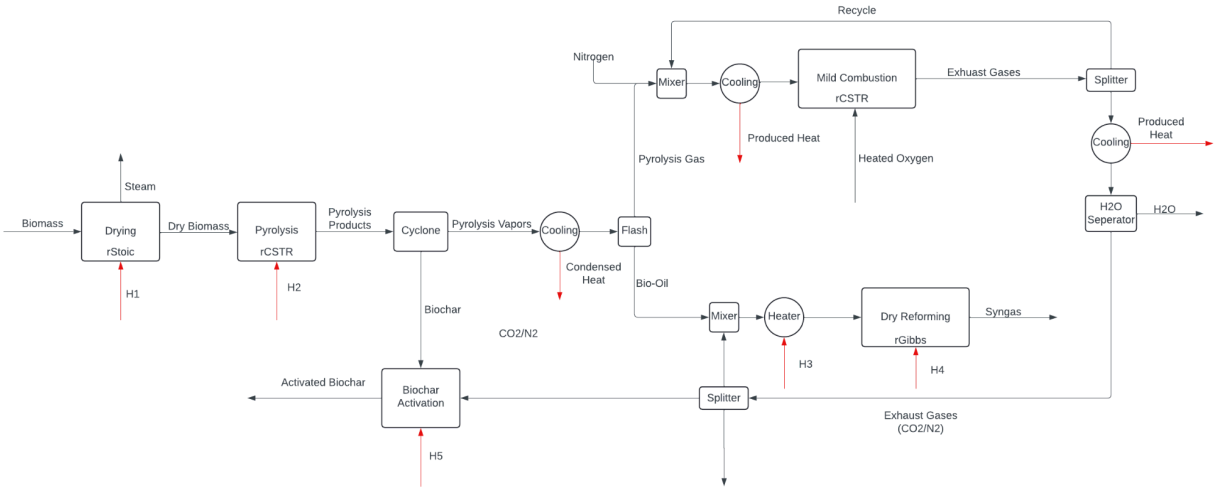

Figure 2: The Aspen Plus flowsheet, Configuration 1. The chosen reactor for each process in Aspen plus. Where heat input is necessary and where heat is produced in the process.

Several process flowsheets have been designed in order to find the most effective usage of energy and carbon sequestration. Although, the main process can be divided into three different sections: the drying and pyrolysis, the Mild combustion and the CO2 reforming, which can be seen in Figure 2.

The first step of the process is to enter the composition of the biomass in the incoming stream. The biomass compounds needed to be entered can be seen in Table 2 under “Biomass Components”. In the supporting information of Debiagi et al (2015) specific compositions for several types of biomass can be found, therefore providing the possibility to analyze the process for different types of biomass sources. The second step is that the biomass enters a dryer, a rStoic reactor in Aspen Plus, the dryer heats the incoming biomass to 150 °C which evaporates the water within the biomass. The water is then removed. The now dry biomass enters the pyrolysis reactor or as used in this model a continuous stirred tank reactor (rCSTR). The CSTR reactor in Aspen Plus allows for entering specific kinetics for the biomass components decomposition. Aspen Plus uses Arrhenius kinetics which is based on the fact that reactions happen when reactant molecules collide with sufficient energy to overcome the activation energy. The rate of reaction is governed by the Arrhenius equation shown as equation 1.

$$k = A * e^{(-E_a/RT)} \quad (1)$$

For equation 1, the variable A represents the pre-exponential factor or frequency factor, which indicates the frequency of collisions between reactant molecules. E_a is the activation energy, representing the minimum energy required for a reaction to take place. R is the universal gas constant and T is the

temperature. This temperature dependence is because at higher temperatures, more molecules possess the necessary activation energy, leading to more frequent collisions and a higher reaction rate. The stoichiometric reactions and the parameters A and E_a used for the thermal degradation of the biomass components were taken from the extensive work carried out by Ranzi, Debiagi and Frassoldati (2017), but without the use of metaplastics. As mentioned previously Aspen Plus was originally designed for the petroleum industry dealing primarily with gases and liquids; it can struggle to handle a solid biomass component as used in this thesis. This becomes a problem because the reacting phase of the component has to be selected for the kinetics and the reactor. For this simulation the selected option for the reacting phase was "liquid phase" and for the CSTR "liquid only" was chosen. The pyrolysis reactor is set to a certain residence time and temperature to mimic a fast pyrolysis, then the program calculates the needed energy for heating up the components as well as the energy needed for reaction.

After the pyrolysis reactor, the produced products consist mostly of the components found in Table 2 under "Biomass Pyrolysis End-Products". These compounds either in solid or vapor form enter a cyclone which effectively separates the biochar and any additional solids from the pyrolysis vapors. The pyrolysis vapors are then cooled down to 20 degrees in the first heat exchanger, this separates the compounds into bio-oil and the pyrolysis gas. However, they are still in the same stream. The flash then separates the pyrolysis gas and the bio-oil into two separate streams, the pyrolysis gas goes to the Mild combustion and the bio-oil goes into the CO2 reforming.

Following the separation, the pyrolysis gas proceeds to the mixer, where it mixes with previously recycled exhaust gases and nitrogen gas. The significance of recycle will be discussed in section 4.2 Mild Combustion Verification. Subsequently, the gas mixture is cooled to reach the autoignition temperature for this process of 1000 °C, as a requirement for the Mild Combustion. Additionally, heated oxygen is introduced into the combustion chamber to initiate the combustion process. As for the pyrolysis, a CSTR is used for the combustion, meaning the necessity for kinetics. While extensive kinetic data with many radical reactions was available, it was deemed excessive for this study, which primarily focuses on energy production. As a result, simplified kinetics were developed and implemented into the CSTR, with all pyrolysis gas species assumed to fully react into CO2 and H2O when given sufficient oxygen supply. The parameters A and E_a used for the arrhenius kinetics were systematically altered until they had an autoignition temperature in the CSTR of around 700 degrees. The CSTR parameters were set to a duty of 0 and a pressure of 1 bar, enabling analysis of the outgoing exhaust stream temperature to ensure it remains within the Mild combustion range. Adjustments such as decreasing oxygen or diluting with N2 in the reactor may be required if the temperature exceeds this range. The exhaust stream is then split, one being recycled back into the mixer and subsequently the Mild combustion. The other stream condensed in a heat exchanger allowing for the removal of water. The now water-free exhaust gases enter another splitter which splits the specific exhaust stream according to the most optimal H2/CO yield with a ratio of 1:1 found in Appendix A.

One of these water-free exhaust streams goes to the CO2 reforming and is mixed with the bio-oil, this mixture is heated in a heat exchanger before entering the CO2 reforming reactor, which is modeled as a rGibbs reactor. The utilization of a Gibbs reactor is necessitated by the absence of known kinetics, complex stoichiometric balances, and competing reactions such as steam reforming, thermal degradation,

and CO2 reforming as was shown in Table 1. The Gibbs reactor eliminates the requirement for precise knowledge of kinetics and stoichiometric balances, instead using chemical and phase equilibrium through Gibbs free energy minimization. Potential products are specified as CO2, CO, H2O, H2,N2 and char. The reactor operates at a specific temperature for optimal yield found in Appendix A and with a constant pressure of 5 bar. From the rGibbs reactor comes out the finished syngas product.

Some of the exhaust gases not going into the CO2 reforming instead goes into the CO2 Activation of the biochar, while the rest ends up as waste. However, only the heating of the biochar and exhaust gases to 900 °C were modeled for the biochar activation.

3.1.2 Model Components

The model components in this process were inspired by the work carried out by Gorensek, Shukre and Chen (2019) which included a total of 49 species. All of the components are shown in Table 2, taken from Gorensek, Shukre and Chen (2019). The first column contains the compound and the second column describes the component ID used in the model. The components are divided into two types; "conventional" (fluid or gas), these components take part in vapor-liquid equilibrium (VLE) and the second type "solid", these solid components do not participate in VLE. The fourth column lists the names of the compounds that have defined properties in the Aspen Plus data bank. Most of the "solid" type species are lacking these properties in the database and had to be manually entered. Finally, the last column describes the chemical formula for the components and for the polymeric biomass species only the monomeric building block.

Table 2: Description of the chemical compounds inserted into Aspen Plus.

Chemical Compound	Component ID	Type	Component name	Formula
Biomass Components				
Tannin	TANN	solid		C15H12O7
C-rich lignin	LIGC	solid		C15H14O4
O-rich lignin	LIGO	solid		C20H22O10
H-rich lignin	LIGH	solid		C22H28O9
Triglyceride	TGL	conventional		C57H100O7
Hemicellulose-Glucomannan	GMSW	solid		C5H8O4
Hemicellulose-xylan	XYHW	solid		C5H8O4
Cellulose	CELL	solid		C6H10O5
Ash	ASH	solid	CALCIUM-OXIDE	CaO
Moisture	H2OL	conventional	WATER	H2O
Biomass Pyrolysis Intermediate Species				
Secondary lignin intermediate	LIG	solid		C11H12O4
C-rich lignin intermediate	LIGCC	solid		C15H14O4
H/O-rich lignin	LIGOH	solid		C19H22O8

intermediate				
Activated hemicellulose 1	HCE1	solid		C5H8O4
Activated hemicellulose 2	HCE2	solid		C5H8O4
Activated cellulose	CELLA	solid		C6H10O5
Tannin intermediate	ITANN	solid		C8H4O4
Biomass Pyrolysis End-Products				
Char	CHAR	solid	CARBON-GRAPHITE	C
Sinapyl aldehyde	FE2MACR	conventional		C11H12O4
Free fatty acid	FFA	conventional	LINOLEIC-ACID	C18H32O2
High-molecular-weight lignin	HMWL	solid		C24H28O4
Glyoxal	GLYOX	conventional	GLYOXAL	C2H2O2
Ethylene	C2H4	conventional	ETHYLENE	C2H4
Acetaldehyde	CH3CHO	conventional	ACETALDEHYDE	C2H4O
Acetic acid	ACAC	conventional	ACETIC-ACID	C2H4O2
Glycol aldehyde	HAA	conventional	GLYCOL-ALDEHYDE	C2H4O2
Ethanol	C2H5OH	conventional	ETHANOL	C2H6O
Acrolein	ACROL	conventional	ACROLEIN	C3H4O
n-propionaldehyde	ALD3	conventional	N-PROPIONALDEHYDE	C3H6O
3-hydroxypropanal	C3H6O2	conventional		C3H6O2
Furfural	FURF	conventional	FURFURAL	C5H4O2
Xylosan	XYLAN	conventional		C5H8O4
Levoglucosan	LVG	conventional	LEVOGLUCOSAN	C6H10O5
Phenol	PHENOL	conventional	PHENOL	C6H6O
5-hydroxymethyl-furfural	HMFU	conventional	5-HYDROXY-METHYLFURFURAL	C6H6O3
Anisole	ANISOLE	conventional	METHYL-PHENYL-ETHER	C7H8O
p-coumaryl alcohol	COUMARYL	conventional		C9H10O2
Formaldehyde	CH2O	conventional	FORMALDEHYDE	CH2O
Formic acid	HCOOH	conventional	FORMIC-ACID	CH2O2
Methane	CH4	conventional	METHANE	CH4
Methanol	CH3OH	conventional	METHANOL	CH4O
Carbon monoxide	CO	conventional	CARBON-MONOXIDE	CO
Carbon dioxide	CO2	conventional	CARBON-DIOXIDE	CO2
Hydrogen	H2	conventional	HYDROGEN	H2
Water	H2O	conventional	WATER	H2O
Non-biomass Components				
Argon	AR	conventional	ARGON	Ar
Nitrogen	N2	conventional	NITROGEN	N2
Oxygen	O2	conventional	OXYGEN	O2

3.1.3 Thermodynamic Framework

The thermodynamic analysis method selected is the Peng-Robinson cubic equation of state, combined with the Boston-Mathias alpha function known as PR-BM within Aspen Plus. While this method was mostly tailored for hydrocarbon and light gases used in the petroleum industry, it has been adopted for researching and modeling the biomass pyrolysis process. However, for the PR-BM to work there is the need to add certain properties for the solids, which are not included in the database as they are for the conventional properties. The properties needed to be included are standard solid heat formation, molecular weight, solid molar volume model parameters and solid molar heat capacity. Some properties for a few conventional components that were not included in the Aspen Plus database were added. These properties included molecular weight, critical temperature, critical pressure, acentric factor, vapor pressure, ideal gas standard state heat of formation, and ideal gas molar heat capacity (Gorensek, Shukre and Chen, 2019).

3.1.4 The Entered Properties

The entered properties are extensively explained in Gorensek, Shukre and Chen (2019).

First the standard heat of formation needed for the solid compounds can be estimated based on the heat of combustion of that compound from experimentally known data. According to Gorensek, Shukre and Chen (2019), if the heat of combustion is unknown, there is a possibility to estimate it based on the heat of combustion per mass unit for any member of the class of that compound.

Secondly, the heat capacity polynomial, also based on the assumption that the heat capacity per unit mass remains the same for a specific class of compounds. This means that the molar heat capacity for a specific member within that class can be estimated by multiplying the mass-based heat capacity of any other member by its molecular weight. In equation 2 the heat capacity polynomial used by Aspen Plus be seen where T represents temperature, C_i are coefficients that vary depending on the material and the range of temperatures being considered in the specific heat capacity polynomial equation.

$$Cp = C_1 + C_2T + C_3T^2 + \frac{C_4}{T} + \frac{C_5}{T^2} + \frac{C_6}{\sqrt{T}} \quad C_7 \leq T \leq + C_8 \tag{2}$$

The solid density polynomial information for the biomass components is scarce according to Gorensek, Shukre and Chen (2019), an assumption was made that the density is the same as starch and is constant even at different temperatures. The starch density was the basis of the molar density for all solid compounds entered. In Equation 3, the solid density polynomial or the solid volume polynomial used by Aspen Plus can be seen, where T represents temperature and C_i are coefficients that vary depending on the material and the range of temperatures being considered. It is important to note that the solid density polynomial and the solid volume polynomial are directly related, as changes in density with temperature correspond to changes in volume. To clarify since the density was assumed to be constant only C_1 was entered.

$$V = C_1 + C_2T + C_3T^2 + C_4T^3 + C_5T^4 \quad C_6 \leq T \leq + C_7 \tag{3}$$

Lastly, some parameters need to be added for some of the conventional fluid not found in the Aspen plus database. For 3-hydroxypropanal, triglyceride, p-coumaryl alcohol, sinapyl aldehyde and xylosan the added properties included molecular weight, critical temperature, critical pressure, acentric factor, vapor pressure, ideal gas standard state heat of formation and ideal gas molar heat capacity. It should be noted that this was only a summary of the extensive work done by Gorensek, Shukre and Chen (2019) . The data for standard heat formation, heat capacity polynomial, density polynomial and the properties of the five different conventional species can be found in Table 2 and Table 3 of Gorensek, Shukre and Chen (2019). The sources for the experimental data and the assumptions and calculations utilized for the different parameters.

3.1.5 Calculations

Aspen Plus handles most of the calculations of mass and energy in this thesis. To confirm the energy calculations by Aspen Plus for the compounds, the LHV was calculated and compared to experimental data. LHV or Lower Heating Value is a measurement of the amount of heat released during the combustion of a fuel, subtracting the energy needed for vaporization of the water produced during the process.

To calculate the LHV in MJ/kg using Aspen Plus an rStoic reactor was utilized. The stoichiometric combustion kinetics were entered for the specific compound being analyzed in the rStoic. Stoichiometric oxygen was supplied and Aspen Plus calculated the amount of produced H2O, CO2 and energy. These results were then used to calculate the LHV according to equation 4. Where ΔH_{vap} is 2.442 MJ/kg at 25 °C and 1 atm according to Wiebren De Jong and Ommen (2015) and m_{H2O} is the mass in kg of water produced by the combustion. $m_{compound}$ is the initial mass of the compound being combusted and Q_{stoic} is the calculated energy by Aspen Plus .

$$LHV = \frac{Q_{stoic} - \Delta H_{vap} * m_{H2O}}{m_{compound}} \tag{4}$$

Calculations were also done to see how much of the energy put into the process goes into the wanted products. This can be seen in equation 5, where the energy of the wanted products syngas and biochar is divided by the energy in the biomass and heat input.

$$\eta = \frac{E_{prod}}{E_{tot}} = \frac{E_{syngas} + E_{Biochar}}{E_{biomass} + E_{heat}} \tag{5}$$

4. Results And Discussion

4.1 Pyrolysis Verification And Optimization

For verification that the kinetic-based pyrolysis model functions correctly, it was compared to the experimentally and model-based results of the thermal degradation of cellulose, hemicellulose, and lignin presented in (Ranzi et al 2017).

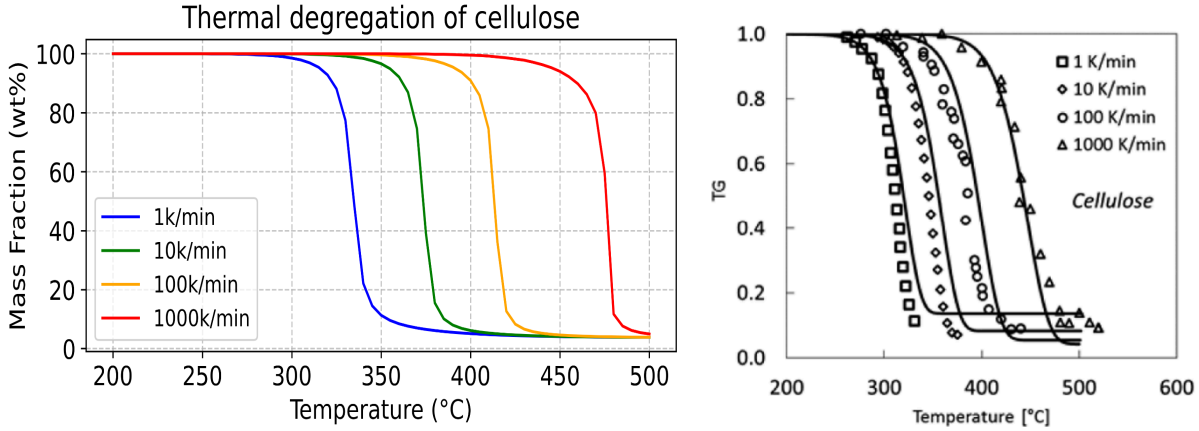

Figure 3. To the left is the predicted thermal degradation of cellulose at different temperatures with specific heating rates. To the right, the experimentally and modeled values predicted in Ranzi et al (2017), where the symbols are the experimental data and lines are the predicted values by the model.

The thermal degradation of cellulose in a CSTR demonstrates a close correlation with the model values from Ranzi et al (2017) as shown in Figure 3. However, the Aspen Plus model predicts a lower solid fraction, indicating less char production during cellulose thermal degradation. The probable reason for this is that Aspen Plus could not accurately replicate the specified heating rate. For instance, a heating rate of 100 K/min implies a residence time of 5 minutes for the cellulose to continuously increase in temperature until it reaches 500°C, a condition not possible in the CSTR as it only uses specific temperature and residence time, and does not provide the option to increasingly change the temperature over time.

To simulate a comparable scenario, a heating rate of 100 K/min translates to 0.6 s/K, indicating that each degree requires a residence time of 0.6 seconds. This residence time was input into the CSTR model while varying the temperature between 200°C and 500°C, producing the results shown in Figure 3. This approach as mentioned resulted in a lower char yield predicted by the model. The outcome obtained was expected because more biochar forms at lower temperatures, and once produced, biochar does not degrade further.

In this model, pyrolysis of incoming cellulose resets with each temperature change. Consequently, at 500°C with a residence time of 0.6 seconds, the model predicts less biochar, as it does not account for the biochar previously formed at lower temperatures. Thus, while the model accurately captures the

degradation intervals, it underestimates the biochar yield. Additionally, the model predicts a similar amount of produced biochar for varying heating rates, whereas, in reality, a 1 K/min heating rate would result in prolonged exposure to lower temperatures and consequently more char production. The verification graph, however, does not account for the initial char formation at lower temperatures when assessing the final char yield at 500°C for a set residence time.

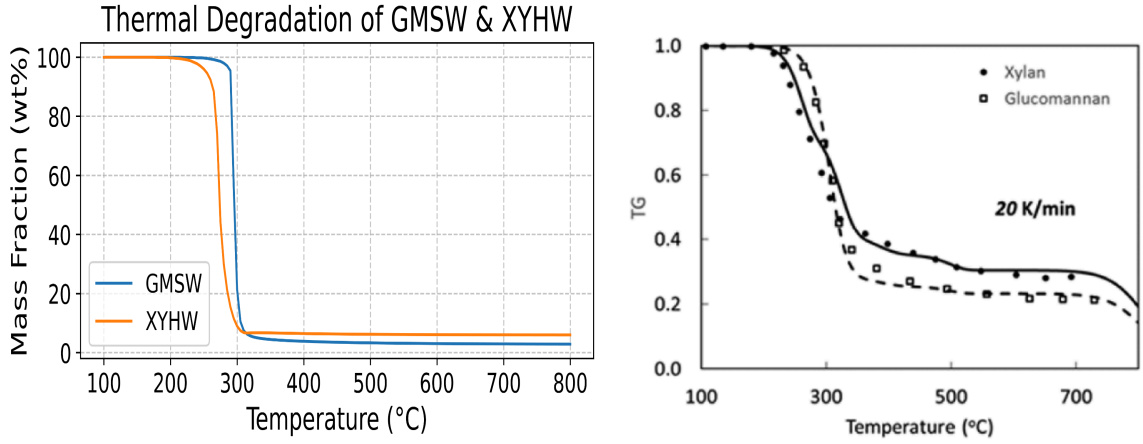

Figure 4. To the left the predicted thermal degradation of glucomannan and xylan at different temperatures with a heating rate of 20K/min. To the right the experimentally and modeled values predicted in Ranzi et al (2017), where the symbols are the experimental data and lines are the predicted values by the model.

Comparing the results for Figure 4 it can once again be seen that the CSTR seems to follow the thermal breakdown of the hemicellulose components, for both the hardwood and softwood. Although compared to the Ranzi model the amount of solid fraction is again underestimated, this is most likely due to the same reasons mentioned for cellulose, and the prediction becomes even worse since hemicellulose leads to higher char production than cellulose thermal degradation as can be seen in the kinetics.

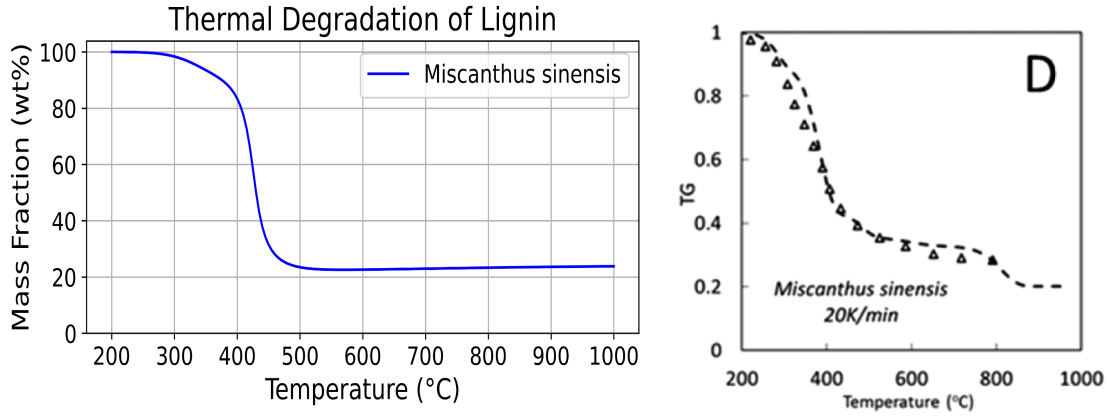

Figure 5. To the left the predicted thermal degradation of lignin at different temperatures with a heating rate of 20K/min. To the right the experimentally and modeled values predicted in Ranzi et al (2017), where the symbols are the experimental data and lines are the predicted values by the model. The lignin model was from Miscanthus sinensis with specific lignin composition ratio found in the work of (Debiagi et al., 2015).

In figure 5 it can be seen that the Aspen Plus model accurately follows the thermal breakdown of lignin compared to the Ranzi model, although once again with a slightly lower char production.

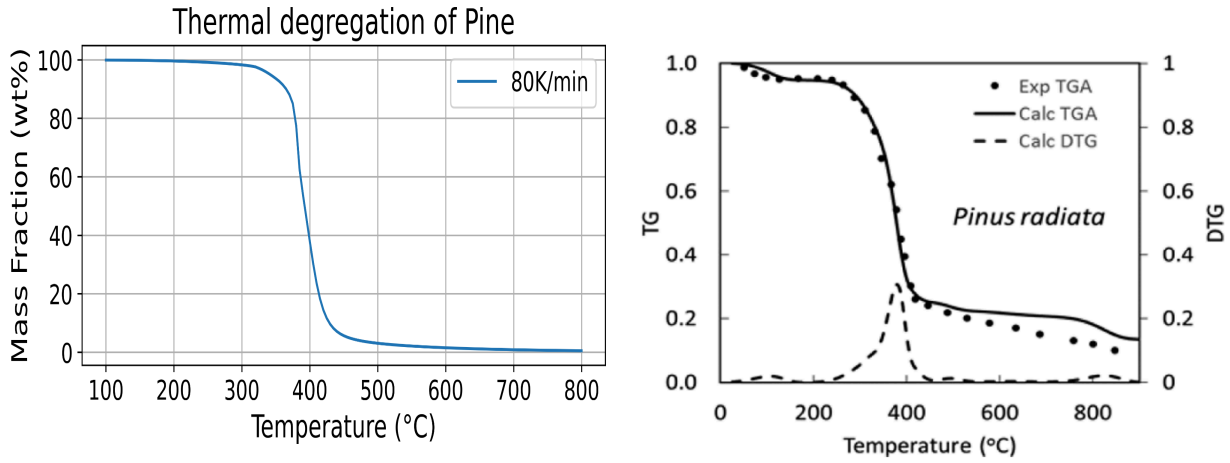

Figure 6. To the left the predicted thermal degradation of Pine at different temperatures with specific heating rates are shown. To the right the experimentally and modeled values predicted in Ranzi et al (2017) with a heating rate of 80k/min, where the symbols are the experimental data and lines are the predicted values by the model.

The thermal degradation in the CSTR as can be seen in Figure 6 seems to follow the thermal degradation of pine in the Ranzi model, but with the lower amount of produced char.

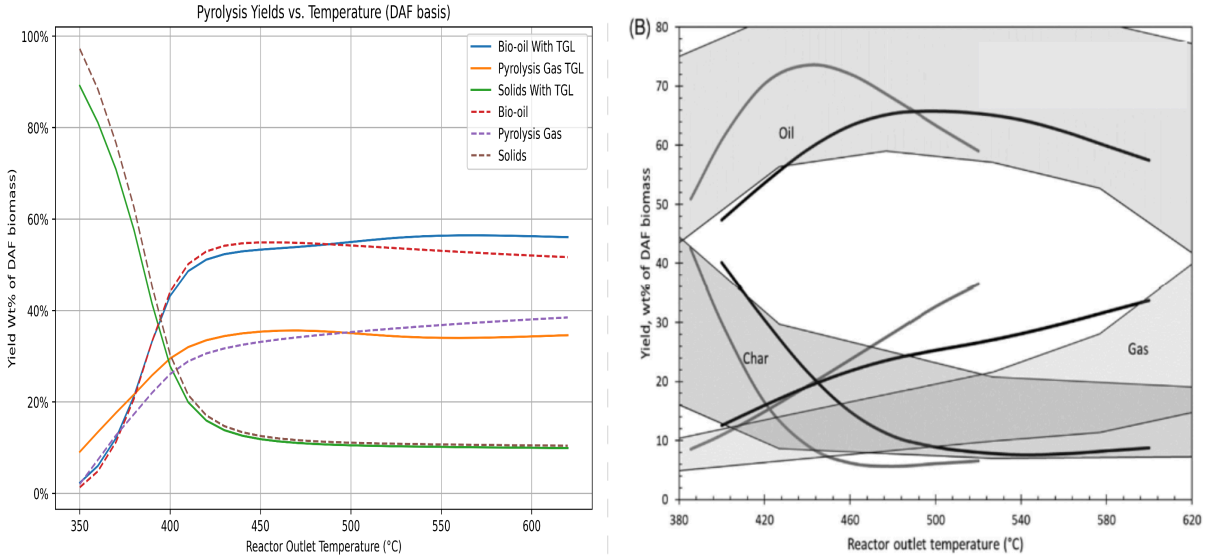

Figure 7. To the left the predicted bio-oil, pyrolysis gas and Solids (biochar), for one simulation with TGL biomass component (Solid lines) and one simulation without (stripped lines). Compared to the simulations made by (Caudle, Gorensek and Chen, 2019) to the right. The gray areas in the graph to the right were experimentally determined yields for softwood by (Calonaci et al., 2010) and the dark lines are the simulated yields by (Caudle, Gorensek and Chen, 2019) and the gray lines the ones simulated by (Humbird et al., 2017) .

To analyze the accuracy of the produced bio-oil, biochar and pyrolysis gas yield, the model was compared to the models by (Humbird et al., 2017),(Caudle, Gorensek and Chen, 2019). The same mass flow and biomass composition found for Douglas fir in Caudle, Gorensek and Chen (2019) was used for the comparison. It should be noted that Caudle, Gorensek and Chen (2019) and Humbird et al (2017) used an ACM with different heat and mass transfer equations for the reactor compared to this study who utilized the standard CSTR in Aspen Plus V.14. In the gray areas in the plot to the right in Figure 11, the experimentally determined yields for softwood by Calonaci et al (2010). For the Aspen Plus simulation for this thesis it was seen that the inclusion of TGL biomass component led to a sudden decline in pyrolysis gas yield around 500°C, something that is not reasonable with increasing temperature. Although it also moved the maximum bio-oil yield to around 550 °C similar to the (Caudle, Gorensek and Chen, 2019) model which included TGL. The accuracy of using the TGL biomass component needs to be further investigated, however, this was not done in this thesis. Instead, without the TGL biomass component the pyrolysis gas component follows the temperature increase more accurately and shifts the maximum bio-oil yield to around 450 °C similar to the simulation by (Humbird et al., 2017) which did not use the extractives TGL and TANN. For a comparison between the experimental yields and the predicted yields by the Aspen Plus model for this thesis, it can be seen that the model accurately follows the temperature's effect on product yields. Same as for Gorensek and Chen (2019) and Humbird et al (2017), the model overpredicts the pyrolysis gas production, however, for this model the predicted bio-oil yield is lower than the other simulations. This is probably due to the usage of ACM for the other authors. Although the bio-oil yield seems to be in range for the experimentally determined values it is on the lower side. Over-predicting pyrolysis gas and underpredicting the bio-oil yield can cause some problems for the rest of the process. Less pyrolysis gas means less energy to the CO2 reforming, and a higher bio-oil amount increases the energy needed for the CO2 reforming. Even though the yields of produced products might be a bit off, the CSTR and kinetics seems to accurately follow the experimental yields for temperature change, and provides the possibility to find the optimal temperature for bio-oil yield for the selected biomass.

4.1.1 Pyrolysis Optimization

Table 3: The Pyrolysis optimization made for Douglas fir for this thesis, with the same biomass composition as used in (Caudle, Gorensek and Chen, 2019).

	Process specification					**Products based on (DAF WT %)**		
	Temperature (C)	***Pressure Pyro (bar)***	***Residence time(s)***	***Pressure Split (bar)***	***Cell/Hcell/Lig Ratio***	***Bio-oil***	***Bio-gas***	***Char***
Baseline	500	2.3	1	5	47/23.5/29.5	51.3	38.9	9.84
Reactor Temp change	400	2.3	1	5	47/23.5/29.5	44.7	34.5	20.8
	450	2.3	1	5	47/23.5/29.5	50.0	39.2	10.9
	550	2.3	1	5	47/23.5/29.5	52.0	38.5	9.53
	600	2.3	1	5	47/23.5/29.5	51.5	39.2	9.35
	650	2.3	1	5	47/23.5/29.5	50.7	40.1	9.25

	1000	2.3	1	5	47/23.5/29.5	48.0	42.8	9.23
Pressure change	500	0	1	5	47/23.5/29.5	51.3	38.9	9.84
	500	0.5	1	5	47/23.5/29.5	51.3	38.9	9.84
	500	1	1	5	47/23.5/29.5	51.3	38.9	9.84
	500	5	1	5	47/23.5/29.5	51.3	38.9	9.84
	500	10	1	5	47/23.5/29.5	51.3	38.9	9.84
	500	50	1	5	47/23.5/29.5	51.3	38.9	9.50
Residence time change	500	2.3	1	5	47/23.5/29.5	50.1	39.6	10.3
	500	2.3	1.5	5	47/23.5/29.5	52.0	38.4	9.64
	500	2.3	2	5	47/23.5/29.5	52.4	38.1	9.51
	500	2.3	2.5	5	47/23.5/29.5	52.7	37.9	9.41
	500	2.3	3	5	47/23.5/29.5	52.9	37.7	9.33
	500	2.3	3600	5	47/23.5/29.5	54.5	37.2	8.25
Pressure split change	500	2.3	1	1	47/23.5/29.5	48.1	42.0	9.84
	500	2.3	1	3	47/23.5/29.5	50.3	39.9	9.84
	500	2.3	1	8	47/23.5/29.5	52.2	38.0	9.84
	500	2.3	1	10	47/23.5/29.5	52.6	37.6	9.84
	500	2.3	1	20	47/23.5/29.5	53.7	36.5	9.84
	500	2.3	1	50	47/23.5/29.5	54.8	35.4	9.85
Cell/Hcell/Lig ratio change	500	2.3	1	5	55/15.5/29.5	53.5	34.6	11.9
	500	2.3	1	5	55/23.5/21.5	53.9	36.7	9.40
	500	2.3	1	5	39/31.5/29.5	47.3	41.3	11.5
	500	2.3	1	5	47/31.5/21.5	50.7	40.1	9.25
	500	2.3	1	5	39/23.5/37.5	46.9	39.2	14.0
	500	2.3	1	5	47/15.5/37.5	50.0	35.9	14.0
Optimization	520	2.3	3	50	47/23.5/29.5	57.3	33.4	9.80

Table 3 provides valuable insights for process optimization. In this thesis, the primary focus is on maximizing syngas production, which necessitates optimizing bio-oil yield. However, Table 3 also offers insights into optimizing char and pyrolysis gas yields if different products are preferred. It is also clear that a temperature increase leads to increased amounts of produced bio-oil and pyrolysis gas while it decreases the amount of produced char. However, a too-high temperature decreases the bio-oil yield and increases the pyrolysis gas yield even further. For the pressure results it is clear that pressure had no significant effect on the different yields. Residence time seems to have an impact on the process yields, a higher residence time lowers the amount of produced biochar and pyrolysis gas while increasing bio-oil yield. These are similar to the results seen in (Caudle, Gorensek and Chen, 2019. Pressure split change

seems to have a significant impact as it increases the bio-oil yield by forcing more of the VLE compounds vapor phase into the liquid phase. Analyzing the effects of the ratio between cellulose, hemicellulose, and lignin on the results shows that high cellulose content increases bio-oil yield, hemicellulose favors pyrolysis gas production, and lignin favors char production. These findings align well with existing literature, supporting that the model behaves as reality. To optimize bio-oil yield, an ideal process would involve maintaining a temperature around 500°C, a slightly longer residence time, and a higher pressure split. Additionally, selecting a feedstock high in cellulose would be beneficial. It is important to note that an excessively high split pressure could result in insufficient pyrolysis gas for Mild combustion, thereby not producing enough heat needed for the CO2 reforming process. This consideration needs to be taken into account for an optimal process.

4.2 Mild Combustion Verification

As mentioned in the method section and can be seen in the process flowsheet, the simulation of the Mild combustion was done with a CSTR, which means there was a need for kinetics. While no simplified kinetics could be found they were made up to simulate that of an autoignition temperature for pyrolysis gas. To simulate autoignition the kinetics were assumed to fully react to CO2 and H2O if enough oxygen was provided, and sufficient high temperature with a 1 second residence time in the CSTR. Sies and Mazlan Abdul Wahid (2020) mention that a temperature of around 700°C is a general autoignition temperature for biogas, although it might depend on the composition of the gas. The kinetics follow the arrhenius power law and the kinetics were set to Ea of 40000 cal/mol and A 1e9s^{-1} value for all compounds.

While in reality the components within the pyrolysis gas will have different autoignition temperatures, the assumption was made that all the components follow the autoignition temperature of a general pyrolysis gas for easier modeling. To be able to analyze the autoignition temperature from the assumed kinetics, sufficient oxygen was applied as well as nitrogen of 309 kg/hr. The temperature of the incoming gas mixture into the CSTR was changed in order to be able to see at what temperature the autoignition would occur for this mixture at a residence time of 1 second. This was conducted for two cases, one with the recycle of the exhaust stream and one without, in order to see the possible effect of the recycle on the autoignition temperature. As can be seen from Figure 8 to the left (without recycle), the reaction started slowly to produce CO2 around 700°C and a clear autoignition temp at 810°C for our proposed kinetics which was deemed as reasonable results since the mixture had a higher ratio of nitrogen then that of normal air.

In Figure 8 to the right are the results for the plot made for the configuration with recycle of the exhaust gases, to see the possible impact of the recycle on the autoignition temperature. It should be mentioned that Aspen plus did not manage to complete the calculations for the recycle graph without errors. This means that the recycle did not converge within the 1e-6 limit. However, it can still provide some insight to the difference between the autoignition temperature for the recycle configuration and the one without. It can be seen that the recycle configuration plot has a wider autoignition temperature, between 700 °C 1000 °C, the reason for this is most likely due to the changing ratio of nitrogen/exhaust gases and fuel due to the recycle. The change in ratio between pyrolysis gas and inert reacted gases/nitrogen becomes so low that the autoignition temperature increases. Because of this, the Mild combustion did not converge until

1000 °C. For this reason, the inlet temperature was set to 1000 °C for the recycle configuration to ensure complete combustion even though arguably it might be higher than that of a classical autoignition temperature for Mild combustion.

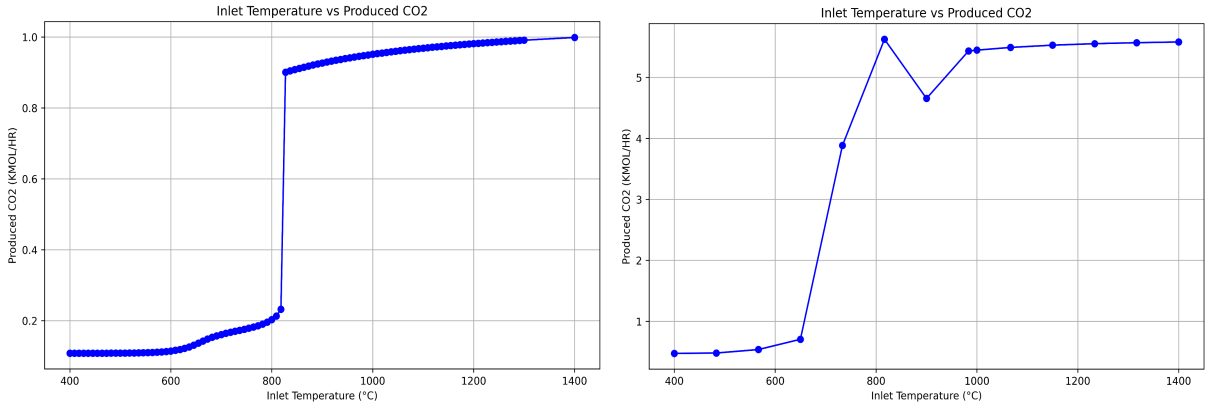

Figure 8: To the left the assumed autoignition temperature made for no-recycle , showing the CO2 production spiking around 810 °C. To the right the assumed autoignition temperature graph for the recycle, showing CO2 production spiking between 700-1000 Celcius.

The next step was to make an oxygen inlet analysis that serves two functions: it provides insight into what oxygen content can be used for the simulation to stay within Mild combustion limits, as well as ensuring that the curve behaves correctly according to experimental data. While no equivalence graph could be found for pyrolysis gas one for methane was used for comparison. From Figure 9 it can clearly be seen that the model behaves like the experimental results in the methane graph Lou et al (2012). There is a temperature increase of the outlet stream with increasing oxygen content in the reactor. This is until oxygen is no longer a limiting factor. When excess oxygen is supplied it instead drives the temperature of the outlet stream down as energy is taken from the exothermic reaction to heat up the oxygen to the temperature of the exhaust. The reason for the lower exhaust temperature in this simulation is simply due to the recycle.

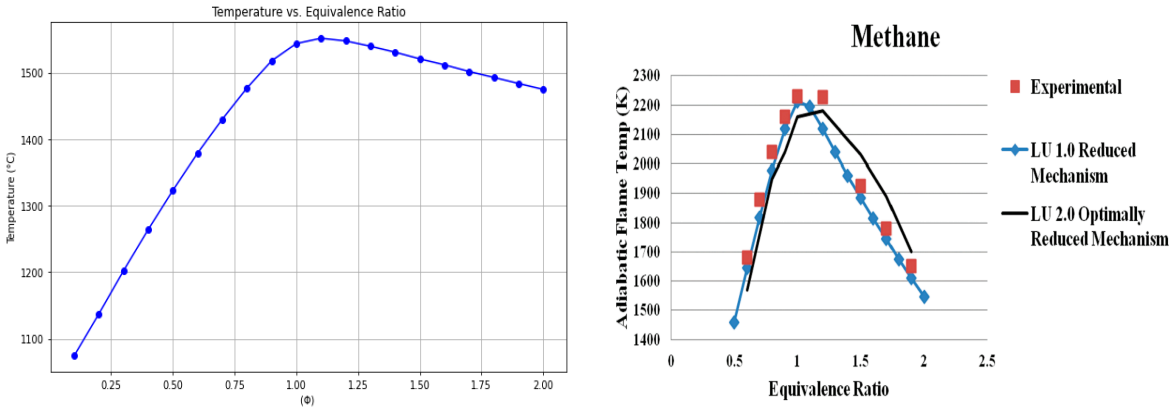

Figure 9: To the left the temperature vs equivalence ratio for the pyrolysis gas. To the right the experimentally determined for methane by Lou et al (2012).

From Table 4, it is clear that by not recycling the exhaust gases, the temperature breaches the Mild combustion limitation of around 2000 K for the pyrolysis gas with an autoignition temperature of around

1000 K. It was also seen that if further nitrogen was added in order to keep the temperature down for the non-recycle, it led to a large amount of unreacted pyrolysis gas. Therefore the recycle was deemed as the best option for this process. Several split fractions were evaluated for the recycle but it was seen that a recycle of 80% allowed the temperature to stay within the Mild combustion limit. Although it should be mentioned that this is not a perfect optimization, there might be a more optimal nitrogen flow for a certain recycle ratio that provides better conversion efficiency and matches exactly the limit of the Mild combustion temperature. In conclusion, the model successfully works in evaluating how much energy can be gained from the system and whether alterations are needed for the oxygen or nitrogen flow to stay within the limit of the Mild combustion.

Table 4: The outlet temperature of the exhaust gases for the model with recycle CSTR and the one without

	Outlet temperature K
Recycle CSTR	1893
No recycle CSTR	2520

4.3 CO2 Reforming Verification

The results of implementing rGibbs for the CO2 reforming can be seen in Figure 10. It follows the general trend of the experimental results made by Landa et al (2023c) which also stated that a temperature of between 600 to 800 °C led to an increase in CO2 conversion. However, it needs to be mentioned that their experiments were made with a catalyst. In Appendix A the trend of increasing the CO2/C yield led to an increase in CO production, something that also was determined by Landa et al (2023c). The reduction in coke formation with temperature above 700 degrees was also shown in Landa et al (2023c) with a slightly higher CO2/C ratio of 1.1 compared to a CO2/C 1 used in figure 10. Similar results were found by Fu et al (2016) but with starting CO2 conversion at 500 °C, however, this difference could be due to the fact that there were no water present in the bio-oil for the experiment done by (Fu et al., 2016), making it a pure dry reforming compared to the bio-oil simulated by Aspen plus which contained water. This gives some verification of the accuracy of the rGibbs. It can be seen that around 800 °C the wanted ratio of H2/CO 1:1 is reached. Significantly it can be seen that below 900 °C char (coke) is still produced. According to the results from the rGibbs there is a trade off between the choice of getting a too high compositional yield of CO in the syngas or losing a little of the syngas yield and producing coke instead.

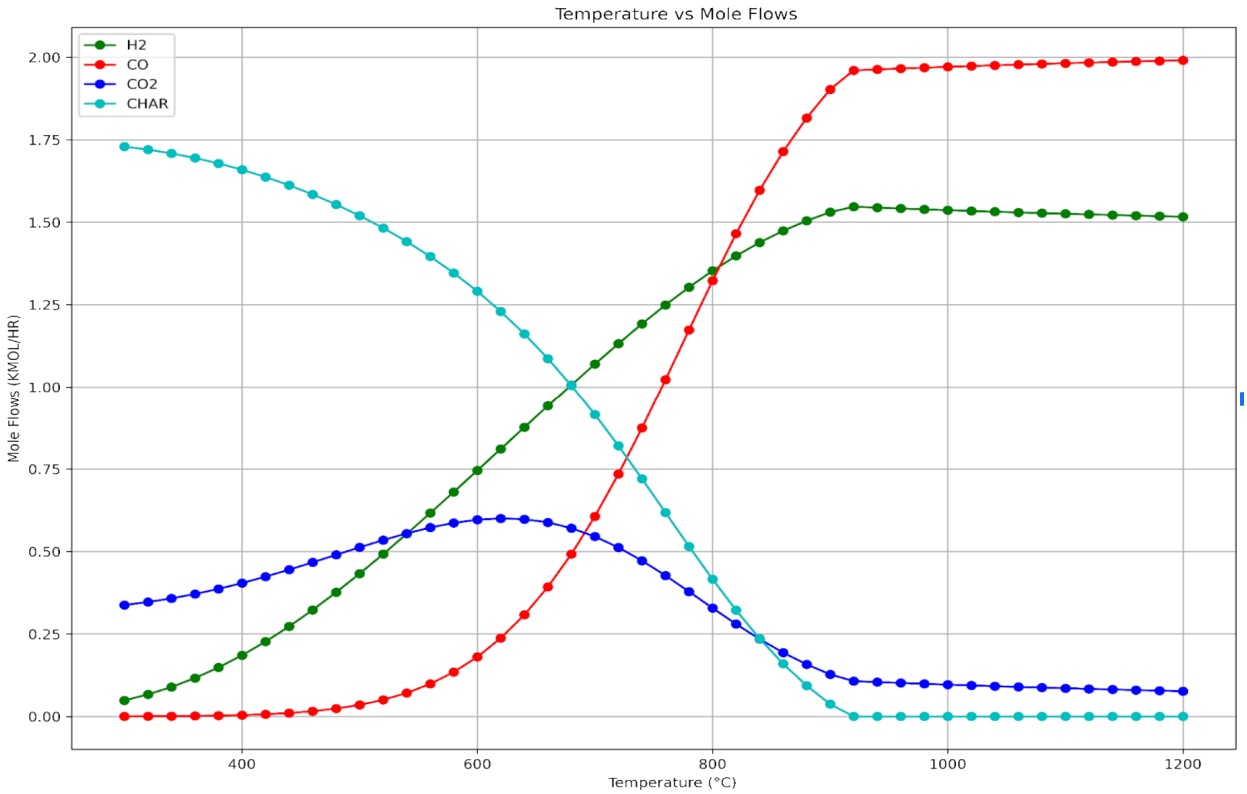

Figure 10. The reactor temperatures effect on Mole flows for the CO2 Reforming made for configuration in Figure 2, with a CO2/C ratio of 1:1. The red line represent the CO mole flow, the green is the H2 mole flow and the dark blue is the is the CO2 mole flow and the light blue is the Char (coke)

Overall, the comparison between the results produced for this thesis and those from other researchers' simulations and experiments shows that a successful model of the process was created. The model provides the possibility to enter a composition of the used biomass and be able to analyze temperature and residence time that gives the optimal bio-oil yield. The model is then able to give the expected outlet temperature from the Mild combustion, thus letting the user know if the combustion stays within limits. Furthermore it provides the possibility for the user to manually change oxygen and nitrogen concentrations in order to find a concentration that maximizes conversion for pyrolysis gas while staying within Mild combustion temperature. The usage of the CSTR and kinetics allows the user to take a sample of the experimentally produced pyrolysis gas, check the real autoignition temperature, and then adjust the kinetics accordingly for a more accurate process description of the Mild combustion. While the CO2 reforming seemed to follow the experimental results of (Landa et al., 2023c) quite accurately, more experimental results need to be done to get a more accurate description of possible energy requirements for a thermal CO2 reforming. The model weakness is the inaccuracy of pyrolysis. While it seems to work to find the optimum bio-oil temperature the amount of pyrolysis gas produced seems to be a bit high and the bio-oil a bit low compared to experimental data. This could impact the possible energy production from the Mild combustion and therefore the amount of energy being able to go into CO2 reforming and the possible syngas yield.

4.4 Configuration Evaluation

To be able to answer the aim of this project three different configurations were evaluated against each other looking at the differences in carbon and energy flow, potential carbon sequestration of the process, and how much carbon goes into the wanted syngas H2/CO.

4.4.1 Configuration 1

Configuration 1 is the same one as extensively described in the method section and can be seen in Figure 2.

One of the main aims of this thesis was to analyze the process impact on the C-cycle and to track the carbon flow throughout the different steps of the process. To achieve this a Sankey diagram was created for the base case of Douglas fir as can be seen in Figure 11, illustrating the flow of 41.4 kg/hr of carbon starting from the biomass and ending in syngas, CO2 and biochar. When analyzing Figure 11 it is clear that most of the carbon ends up in the bio-oil and pyrolysis gas. This was expected for fast pyrolysis, whose primary goal is to produce bio-oil. Looking at the outgoing streams in the Sankey diagram, the overall CO2 conversion or carbon sequestration for the system can be calculated. Since all of the carbon inside the biomass was previously CO2 taken from the atmosphere the conversion of CO2 is very easy to look at.

The activated biochar intended to be used as a fertilizer is effectively going to bind 7.8 Kg/hr to the ground which is around 19% of the incoming carbon. For the syngas the amount of bound carbon depends on the utilization of the syngas. The syngas can be used for chemical synthesis, such as producing dimethyl ether (DME) which can be used as alternative fuel to diesel (Kittelson et al., n.d.). However, DME can also be transformed into several different feedstock chemicals, such as acrylic acid which can produce products like plastics, paints and coatings(Kumar and Singh, 2016). Therefore the amount of carbon dioxide sequestered from the atmosphere will highly depend on the synthesis product, its use and recyclability. For the accuracy of the Sankey graph, it is important to note that as syngas cools, its composition changes due to the water-gas shift (WGS) reaction. However, the final composition used for continued synthesis remains consistent with that depicted in the Sankey diagram.

The 21.8 kg/hr carbon going into the CO2 reforming comes out in three different products CO, CO2 and char. The char produced in the CO2 reforming is assumed to lack the properties needed to be utilized in the biochar activation. It is also assumed to not be further processed and is accounted for in the total carbon sequestration. This results in about 49% of the incoming carbon being sequestered in the CO2 reforming. During biochar activation, 13.8 kg/hr carbon goes into the process. There is some uncertainty regarding the extent to which incoming exhaust CO2 binds to the activated biochar and how much CO2 is produced due to the burn-off. For the calculations it was assumed that 80% of the incoming biochar was successfully activated, as referenced in (Franciski et al., 2018). This contributes to approximately 15% of the total incoming carbon being sequestered through CO2 activation. The overall percentages of carbon sequestration and produced CO2 are summarized in Table 5 below.

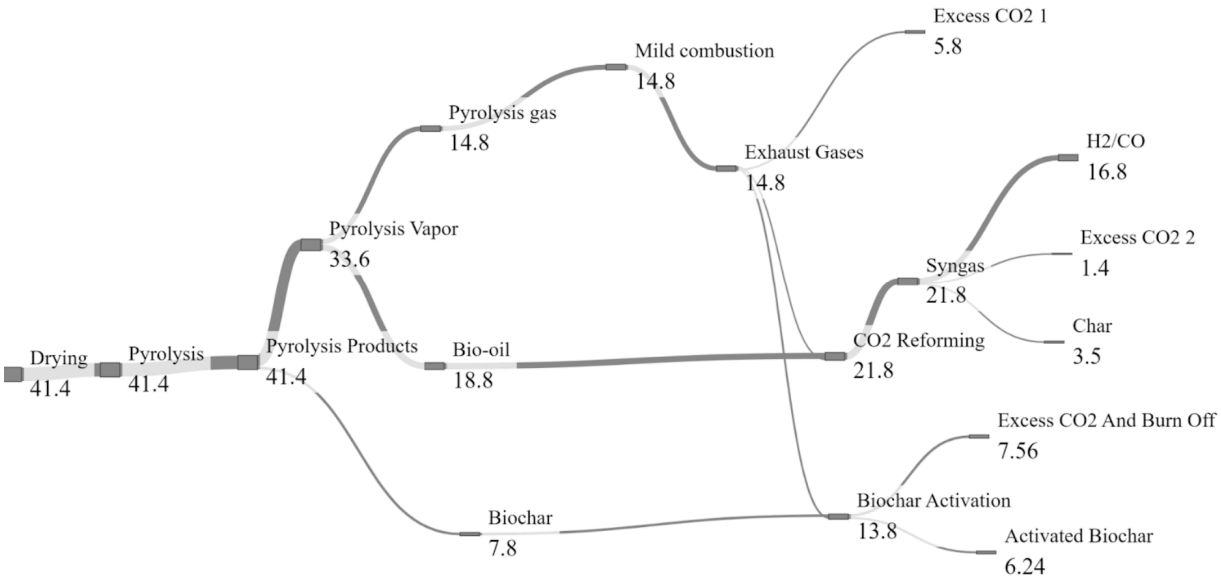

Figure 11: Sankey diagram, illustrating the flow of 41.4 kg/hr of carbon throughout the process for Configuration 1.

To analyze the energy flow throughout the process and determine the energy input for each step, as well as to assess whether any additional energy is required in the form of renewable energy, again a Sankey diagram was utilized. Figure 12 provides an overview of where the energy from the biomass goes in and how much heat is required for each process to take place. The analysis shows that most of the biomass energy and heat input, around 85%, goes into the pyrolysis vapor, while the remaining 15% is in the biochar.

Continuing forward in Figure 12 it can be seen when pyrolysis vapor is cooled down for separation of bio-oil and pyrolysis gas 25.2 kj/s heat is released, this condensing heat can be utilized in the drying process. The energy in the pyrolysis gas and the incoming oxygen is converted into 177.1 kJ/s of heat. This is done through cooling down the exhaust gases in the two heat exchangers depicted as cooling in the Figure 2, this heat can then be transferred to the other processes. Considering the necessary heat input for CO2 reforming, heating of oxygen, pyrolysis, and biochar activation, it seems that the heat produced in the Mild combustion can sustain the other processes within the system. While the temperatures produced in the Mild combustion are high enough to allow heat exchangers to heat up the rest of the processes to their necessary temperatures, further analysis of eventual heat losses and possible heat transfers between the materials would also be necessary to confirm that the energy produced in the Mild combustion is enough for the whole system. Nevertheless, these results are promising.

As depicted in Figure 12 some energy is lost in unburnt pyrolysis gas. Part of which is sent with the exhaust gases into CO2 reforming, however, most is vented out of the system, leading to some wasted energy. This suggests that the reactor's residence time may need to be increased slightly to ensure complete combustion. However, it also highlights the complexity of achieving complete combustion while maintaining the low temperatures required for Mild combustion. Figure 12 also shows that most of the energy, 285.5 kJ/s, goes into the syngas, although it should be noted that 29.5 kJ of this energy is in the form of heat, which is necessary to maintain the H2/CO composition. In practice, the syngas would be

cooled before being sent for further synthesis, allowing this heat to be used elsewhere in the process. It is important to remark that WGS will have an impact on the potential available energy as the composition changes when the syngas cools down. This impact of the WGS was not calculated and the possible available energy to be utilized were therefore omitted.

Lastly, 78.97 kJ/s was utilized in the activation of the biochar. Since the biochar needs to be cooled down slowly to ambient temperature to maintain its complex porous structure, the energy released during this cooling process is assumed to be lost to the surroundings. Additionally, there will be further energy losses due to burn-off during activation. It is assumed that with a 20% burn-off rate, 20% of the initial energy contained in the biochar will be lost.

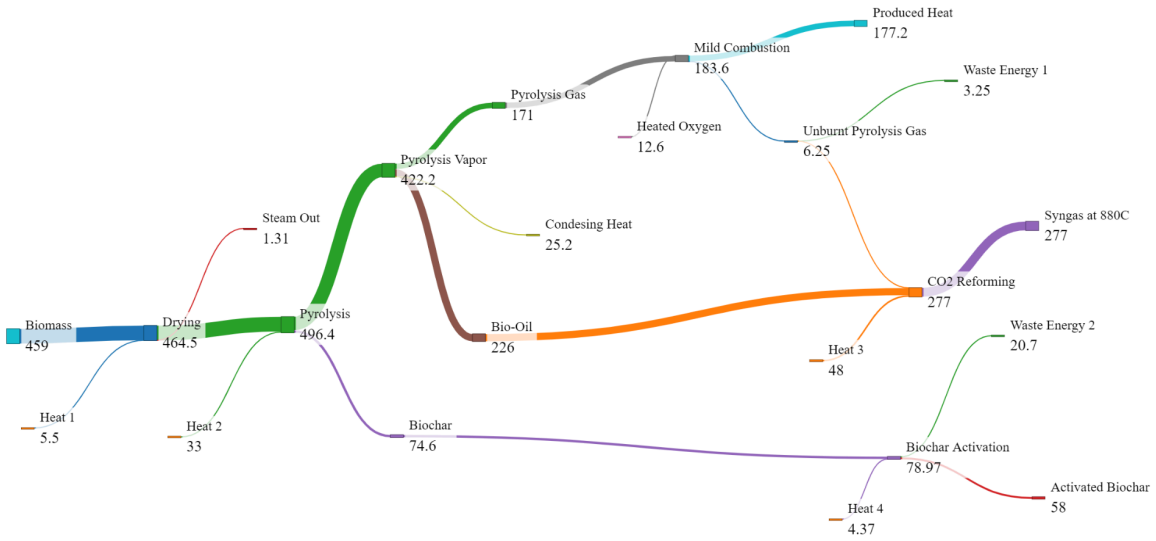

Figure 12: Sankey diagram describing the Energy flow in kJ/s of the process and where and much heat was needed for the different units for Configuration 1.

Table 5 showcases the calculated percentages of carbon flow throughout the process, the total potential carbon sequestration for Configuration 1, the calculated lower heating values (LHV) of the biomass and subsequent products, and the energy distribution derived from the Sankey diagram. It details how much energy was put into the finished products, how much went into heat, and the total energy wasted. Table 5 shows that the total carbon sequestration potential of the whole system reached up to 64%. The energy distribution shows that 55% of that energy went into the syngas (counted with the produced char) and the biochar. 35% went into the produced heat while 10% was accounted for energy loss of the unburnt pyrolysis gas, burn-off and cooling of the biochar. The calculated LHV values give some insight into the energy density of the components and how they differ depending on the process. It also works as a validation for the calculated heat values by Aspen Plus. According to Wiebren De Jong and Ommen (2015) wood pellets with a moisture content of 1-5 wt% has a LHV of 18-24 MJ/KG which seems to match the calculated values of Aspen Plus. For which the biomass had a moisture content of 4.9 wt%.

Wiebren De Jong and Ommen (2015) also mentions that charcoal has a LHV of 30-32 which also seems to be correct to the one calculated for biochar by Aspen Plus. Bio-oil produced in a fast pyrolysis with an initial moisture content of 10% had a 16.5 MJ/kg (Wiebren De Jong and Ommen, 2015) . This is slightly lower than the one calculated by Aspen plus which is probably due to the difference in moisture between the biomasses.

Table 5: This table shows the calculated percentages of carbon flow throughout the process, the total potential carbon sequestration, the calculated energy in the components by Aspen Plus, the calculated LHV values, and the energy distribution into products, heat and waste for Configuration 1 .

Configuration 1	**Carbon (w.t%)**	**Energy (kJ/s)**	**LHV MJ/KG**
Biomass	100	459	18.4
Pyrolysis Gas	30	170	18.2
Bio-Oil	51	226	17.9
Biochar	18	72.6	30.4
End Products	100		
CO2	36	-	-
Syngas	41	256	12.9
Activated Biochar	15	58	30.4
Char	8	-	-
Carbon Sequestration Potential (%)	**Energy Conversion into products (%)**	**Heat Produced (%)**	**Waste Energy (%)**
64	**55**	**35**	**10**

4.4.2 Process Optimization

To assess the impact of process optimization on the syngas yield and its subsequent effect on the C-cycle, the optimization case for maximizing bio-oil production from Table 3 was utilized. Additionally, for syngas production, the optimal temperature and CO2/C ratio were identified in Appendix A. These optimization conditions were then put into Configuration 1 to be able to evaluate its impact on the C-cycle compared to the non-optimized case. Figure 13 shows the effect of the optimized pyrolysis conditions on Configuration 1, it can be seen that more carbon goes into the bio-oil instead of the pyrolysis gas, compared to the non optimized case, subsequently leading to higher syngas production and lower CO2 emissions.

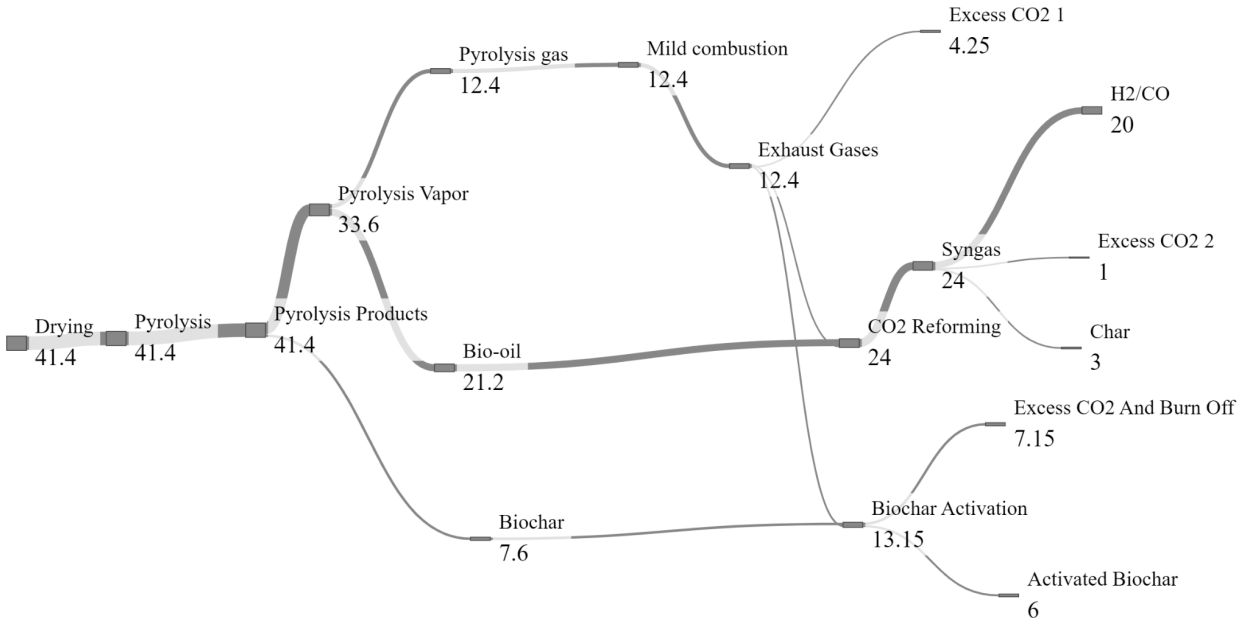

Figure 13: Sankey diagram, illustrating the flow of 41.4 kg/hr carbon throughout the process for Configuration 1 optimization.

Figure 14 reveals that more energy is directed into the produced syngas, while less heat is generated from Mild combustion. This naturally corresponds with the higher production of bio-oil and the lower production of pyrolysis gas. Despite these changes, the results indicate that there is still sufficient heat produced to sustain the rest of the process.

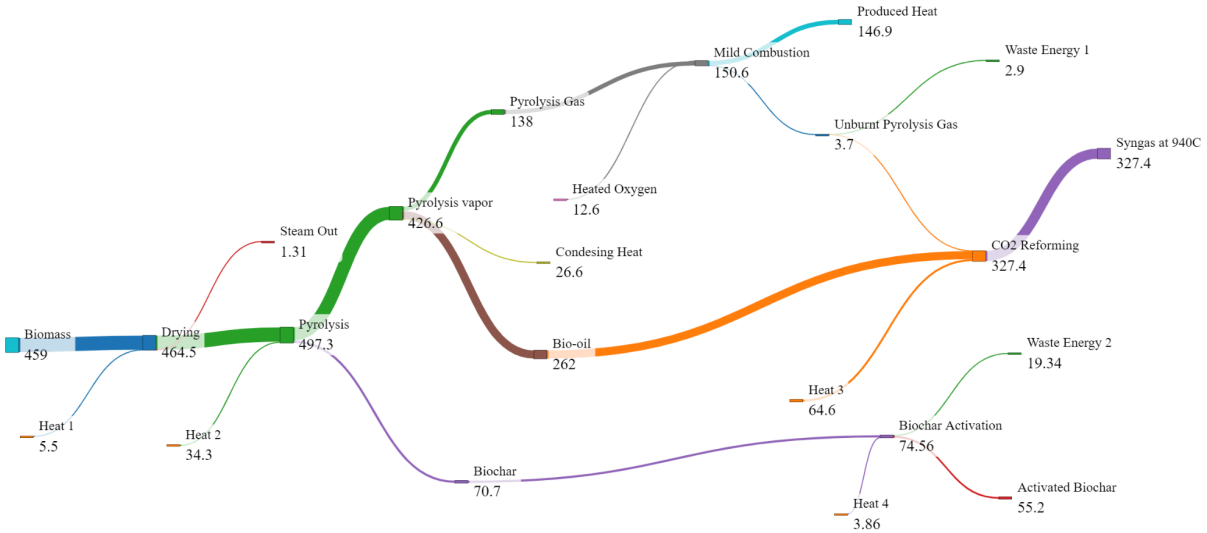

Figure 14: The Energy flow in kJ/s of the process and where and much heat was needed for the different units for Configuration 1 optimization.

.

Examining Table 6 provides a clearer picture of the total impact of the optimization. It reveals an increase in carbon directed towards syngas, resulting in a higher syngas yield compared to the non-optimized case, while also reducing CO2 emissions and causing only a slight decrease in activated biochar yield. This in turn leads to the process having an even larger impact on the C-cycle by making the process even more carbon negative. The optimization also improves the energy conversion into products and increases the LHV of the syngas, something that could be important if it is going to be used as fuel. This underlines the importance of optimizing pyrolysis conditions for bio-oil yield and adjusting the CO2 reforming temperature and CO2/C ratio for maximizing syngas production. It is important to mention that there are further optimization possibilities for maximizing bio-oil yield by switching to a more cellulose-based feedstock, as showcased in optimization Table 3. This change could potentially increase bio-oil yield to up to 70%, as indicated in (Chen et al., 2022). However, such a high bio-oil yield might result in insufficient heat production from Mild combustion. In this scenario, the introduction of energy from renewable resources could be necessary in order to provide enough heat for the process, so that the syngas yield and the carbon sequestration of the process can be maximized.

Table 6: This table shows percentages of carbon flow throughout the process, the total potential carbon sequestration, the calculated energy in the components by Aspen Plus, the calculated LHV values, and the energy distribution into products, heat and waste for Configuration 1 Optimization .

Configuration 1 Optimization	**Carbon (w.t%)**	**Energy (kJ/s)**	**LHV MJ/KG**
Biomass	100	459	18.4
Pyrolysis Gas	30	170	16.4
Bio-Oil	51	226	18.6
Biochar	18	72.6	31.1
End Products	100		
CO2	30	-	-
Syngas	48	293	13.8
Activated Biochar	14	55	31.1
Char	7	-	-
Carbon Sequestration Potential (%)	**Energy Conversion into products (%)**	**Heat Produced (%)**	**Waste Energy (%)**
70	**60**	**30**	**10**

4.4.3 Configuration 2

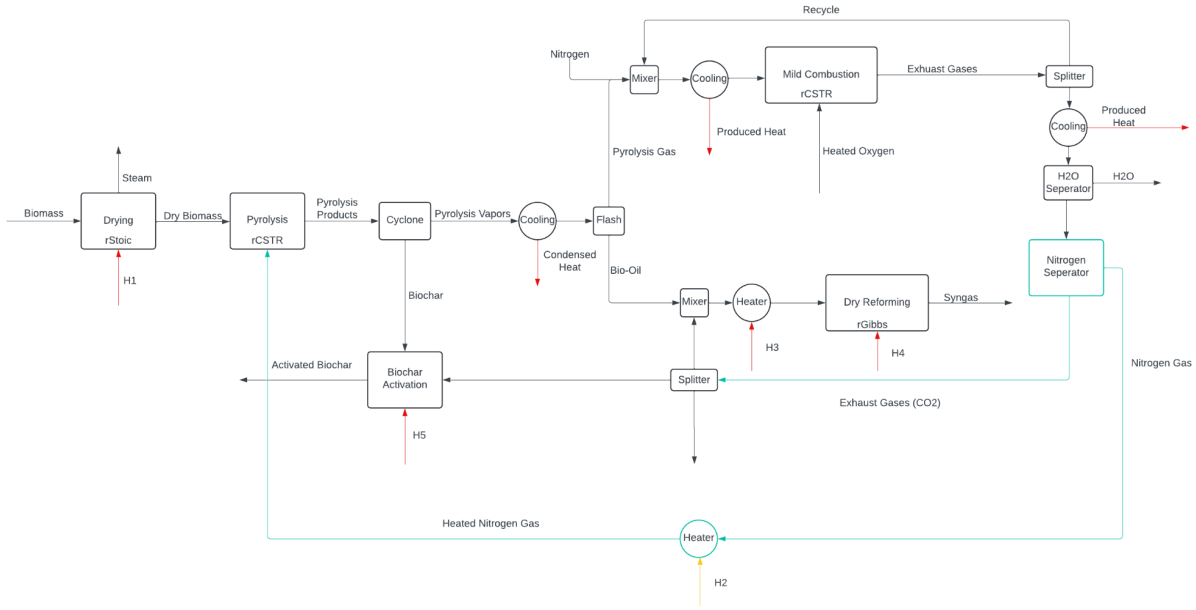

Figure 15: The Aspen Plus flowsheet for Configuration 2. The chosen reactor for each process in Aspen plus. Where heat input is necessary and where heat is produced in the process. H2 is assumed to be from renewable resources. The blue lines represent the changes to Configuration 2 compared to Configuration 1.

Configuration 2 was proposed to evaluate the possibility to use heated nitrogen for heating up the pyrolysis, a common method for pyrolysis of biomass (Jerzak, Reinmöller and Magdziarz, 2022). Different from Configuration 1, nitrogen is removed from the exhaust stream after the Mild combustion. This is a quite difficult process. In the simulation, the energy requirement was estimated for a cryogenic separation by reducing the temperature of the exhaust gases to -170°C. This solution for separating the nitrogen is an energy-requiring process and also necessitates for the nitrogen to be heated back up before entering the pyrolysis. Another problem that occurred was that the nitrogen needed to be heated up to around 2450°C before containing enough energy needed for the pyrolysis. This could probably cause issues for the pyrolysis as the temperature of incoming nitrogen gas is too high. To reduce the temperature, the mass flow of nitrogen could instead be increased. However, this was seen to cause problems in the Mild combustion as the increased concentrations of nitrogen led to lower temperature in the reactor, leading to a lot of unreacted pyrolysis gas. Also a mass increase of nitrogen would lead to higher energy needed for separating the nitrogen from the exhaust stream. In total, even though external energy from renewable resources would be introduced, heated nitrogen for the pyrolysis does not seem to be a viable option for this process. Nevertheless, Configuration 2 carbon flow and energy flow were evaluated to see the process impact on carbon sequestration and energy conversion into products, the Sankey diagrams can be found in Appendix B.

From Table 7 it can be seen that Configuration 2 resulted in a higher amount of produced CO2 and a lower syngas yield, which in turn led to lower carbon sequestration for the overall process. This emphasizes that this configuration not only has design difficulties but also yields poorer results. The increase in gas yield and the lack of significant change in biochar yield coincide with the results made by

(Demiral and Şensöz, 2006). However, the findings by Demiral and Şensöz (2006) suggest that there might be an optimal nitrogen flow rate that could also lead to a higher bio-oil yield instead of a reduced one. Indicating that the nitrogen flow into the pyrolysis process for Configuration 1 could be optimized to enhance bio-oil yield even further, thereby leading to increased carbon sequestration. Notably LHV increased for the syngas but this is simply because the inert nitrogen gas was removed.

Table 7: This table shows percentages of carbon flow throughout the process, the total potential carbon sequestration, the calculated energy in the components by Aspen Plus, the calculated LHV values, and the energy distribution into products, heat and waste for Configuration 2.

Configuration 2	**Carbon (w.t%)**	**Energy (kJ/s)**	**LHV MJ/KG**
Biomass	100	459	18.4
Pyrolysis Gas	40	193	18.3
Bio-Oil	42	204	17.8
Biochar	19	71.9	30.4
End Products	100		
CO2	39	-	-
Syngas	37	235	15.6
Activated Biochar	15	58	30
Char	9	-	-
Carbon Sequestration Potential (%)	**Energy Conversion into products (%)**	**Heat Produced (%)**	**Waste Energy (%)**
61	**50**	**38**	**12**

4.4.4 Configuration 3

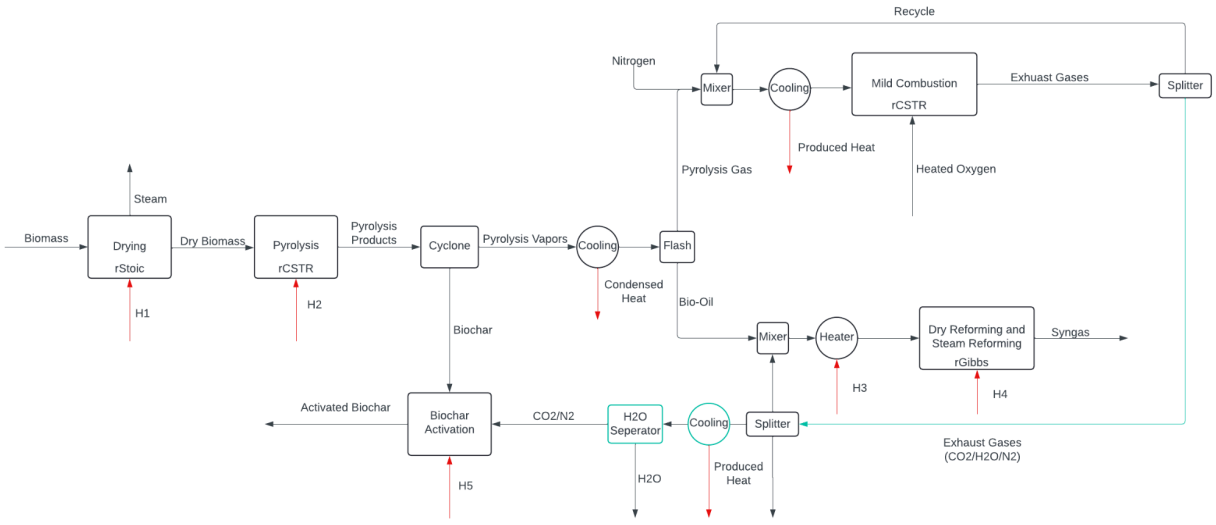

Figure 16: The Aspen Plus flowsheet for Configuration 3. The chosen reactor for each process in Aspen plus. Where heat input is necessary and where heat is produced in the process. The blue lines represent the changes to Configuration 3 compared to Configuration 1.

Configuration 3 was designed to evaluate the possibility of not removing the water from the exhaust gases before sending them to dry reforming. This change transforms the dry reforming process into a mixed steam and CO2 reforming process. Additionally, it reduces the need to cool down the exhaust gases in the heat exchanger before they are sent into CO2 reforming, potentially lowering heat losses. However, water still needs to be removed from the exhaust stream entering the biochar activation stage, so this change does not lower the amount of required units for the system.

In the carbon Sankey diagram for Configuration 3, Figure 17 , it can be seen that this modification had a positive impact on increasing the H2/CO concentrations in the syngas while maintaining the ratio at 1:1. This suggests that a combined steam/CO2 reforming process might be preferable to a pure CO2 reforming process for maximizing syngas yield and decreasing the produced amount of the unwanted char. It is important to note that the water from the bio-oil already prevents the dry reforming from being entirely dry, but not removing the water from the exhaust gases increases the ratio of steam reforming to dry reforming.

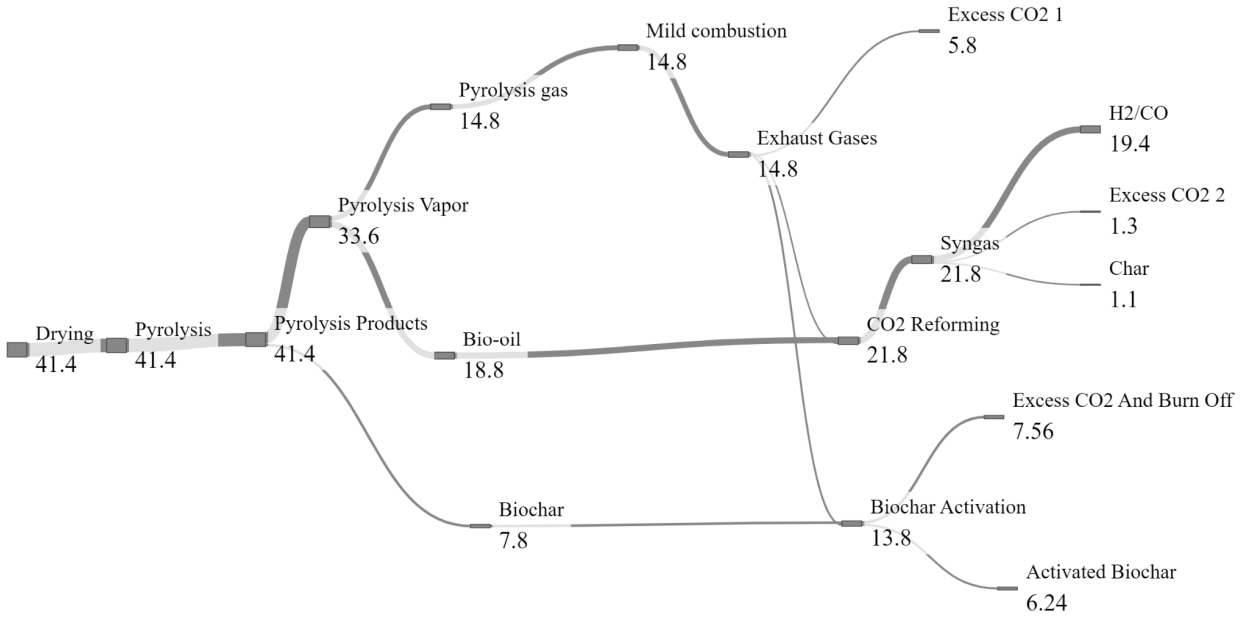

Figure 17: Sankey diagram, illustrating the flow of 41.4 kg/hr carbon throughout the process for Configuration 3.

In Figure 18, the main difference compared to the energy Sankey for Configuration 1 is the fact that the hot exhaust gases go directly into the CO2 reforming process, thereby reducing the energy required in Heat 3 compared to Configuration 1. Also the syngas has a higher amount of energy meaning that the total energy conversion into products goes up as can be seen in Table 8.

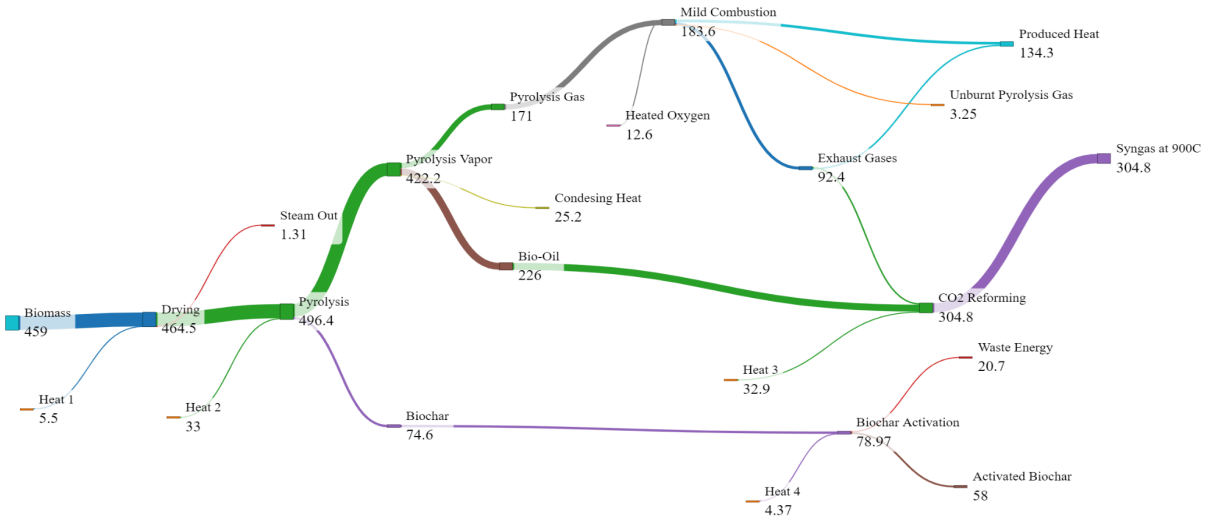

Figure 18: The Energy flow of the process and where and much heat was needed for the different units for Configuration 3.

As already indicated by the results from the carbon flow Sankey diagram, the total carbon sequestration increases as more carbon is directed into the syngas. There is also a slightly lower CO2 output to the atmosphere. Also it can be seen that there is a higher energy conversion into products compared to Configuration 1 and slightly lower wasted energy.

Table 8: This table shows percentages of carbon flow throughout the process, the total potential carbon sequestration, the calculated energy in the components by Aspen Plus, the calculated LHV values, and the energy distribution into products, heat and waste for Configuration 3.

Configuration 3	**Carbon (w.t%)**	**Energy (kJ/s)**	**LHV MJ/KG**
Biomass	100	459	18.4
Pyrolysis Gas	36	170	18.2
Bio-Oil	45	226	17.9
Biochar	19	72.6	30
End Products	100		
CO2	35	-	-
Syngas	47	266	12.9
Activated Biochar	15	58	30
Char	3	-	-
Carbon Sequestration Potential (%)	**Energy Conversion into products (%)**	**Heat Produced (%)**	**Waste Energy (%)**
65	**57**	**32**	**11**

The impact of the steam amount in the CO2 reforming was extensively studied both experimentally and using an RGibbs reactor by (Landa et al., 2023a). The results show that an excessive amount of steam compared to CO2/carbon can lead to reduced CO2 conversion. It was concluded that a CO2/C ratio of 0.5 and a S/C ratio of 0.5 at 900°C resulted in optimal CO2 conversion. This is very similar to the chosen operation conditions for the reforming in Configuration 3. In Appendix A it is shown that for Configuration 3 a temperature of 900°C, a CO2/C ratio of 0.51, and a calculated S/C ratio of 0.43 were chosen for optimal H2/CO yields while maintaining a ratio of 1:1. Additionally, Landa et al (2023a) included CH4 in the rGibbs reactor products, which might lead to more accurate results when considering the kinetics described in section 2.6, compared to not including it in this thesis.

4.5 Process Impact On The C-cycle

To analyze the process impact on the carbon cycle, it can be seen that CO2 is released into the atmosphere from the Mild combustion, CO2 reforming and biochar activation. However, most of the carbon in the process will be the biochar and syngas. Leading all configurations to have a carbon sequestration potential of at least 61% with even higher sequestration possibilities through optimization of the pyrolysis and the CO2 reforming. It also seems that a combined steam/CO2 reforming could improve the total carbon sequestration potential and the syngas yield. Overall the process will impact the C-cycle by removing CO2 from the atmosphere and storing it in the biochar as carbon-based fertilizer, leading to an increased soil-carbonization. The carbon will also be stored in the carbon-synthesized products made from the syngas. This will counteract the man-made CO2 emissions from fossil fuels and stabilize the C-cycle back to a more natural state. However, as previously mentioned how much carbon will be stored in the syngas will highly depend on the usage of the syngas. If it is used as a fuel all of the carbon will be let back out into the atmosphere as CO2, lowering the carbon sequestration capabilities of the process to only the biochar. As mentioned in the background, it is important to take the processing of the feedstock into account if it is transported through fossil-based fuels, it will reduce or completely eradicate the carbon negativity of the process. Therefore, prioritizing locally sourced feedstock to minimize CO2 transportation emissions is essential. Additionally, for true sustainability and for the process to count as carbon negative the biomass must be regrown, emphasizing the importance of using sustainable farming and forestry practices. If the biomass is not regrown the process will instead have an opposite impact on the C-cycle by releasing CO2 into the atmosphere previously contained in the biomass.

Looking at how the energy flow could impact the C-cycle; it seems that all configurations produce enough heat in the Mild combustion and do not necessitate any external energy being input to the process. Although, as mentioned before this would need to be further investigated. Even though the process does not necessitate any use of renewable resources it should be mentioned that grinding of the biomass into small pieces allows for better heat transfer and higher bio-oil yield. Grinding is a very energy intensive process which means that if this energy comes from fossil fuels it could reduce the process carbon negativity (Boylston, 2018). Therefore to keep the carbon negative impact of the process on the C-cycle, introducing renewable energy in this part of the process could be vital. Taking all of this into consideration the process seems promising to create a sustainable C-cycle, while still providing humanity with neccecasy carbon based products.

4.6 Process Impact On The N-cycle

To analyze the process impact on the N-cycle, the areas of the process containing any form of nitrogen were examined. First off, there is some nitrogen in biomass, however, it is a comparatively low amount in lignocellulosic biomass, therefore it was assumed to not be included in this model. Yet, if the type of biomass being used contains more nitrogen, such as manure or food waste, it could be more interesting to look at. Several investigations have shown that fast pyrolysis with a high heating rate will lead to higher amounts of NH3 and HCN formation, while slow pyrolysis with a lower heating rate will lead to the formation of nitrogen in biochar and bio-oil. Since the process requires a fast pyrolysis for maximizing bio-oil yield it can therefore be expected that this HCN and NH3 would mostly go out with the exhaust gases (Xiong et al., 2023).

The second form of nitrogen being put into the process is in the form of nitrogen gas. In the pyrolysis nitrogen gas is used to expel any oxygen coming in with the biomass and in the Mild combustion, it is used as a dilution agent to keep the temperatures lower. This nitrogen gas will exit the process with the syngas and exhaust gases and will not have any impact on the nitrogen cycle. If Configuration 2 is employed the nitrogen will be recycled and not leave the process. As mentioned in the background the major impact on the nitrogen cycle is when nitrogen gas is present during combustion processes at high temperatures since it transforms some of the nitrogen gas to NOx gases. However, since the Mild combustion is used the assumption can be made that very little thermal NOx will be produced and most likely since there is not much nitrogen in lignocellulosic biomass very little fuel NOx can be assumed to be produced as well. Leading to the conclusion that the Mild combustion impact on the nitrogen cycle through NOx production will be minimal.

Lastly, the main impact on the nitrogen cycle will be from the implementation of biochar as a fertilizer. Jindo et al (2020) showed that the use of biochar in combination with nitrogen fertilizer effectively minimized soil nitrogen loss (both gaseous and leaching). Also, it has been shown that biochar can improve N-immobilization of NH_4^+ therefore improving the residence time of the nitrogen in the soil. The biochar also leads to reduced ammonia (NH_3) volatilization which is the main cause of soil-N loss. The increased residence time and reduced volatilization loss lead to an increased uptake of nitrogen by the plant, effectively binding it within the plant. This showcases the nitrogen capture capability of the biochar. Although, it should be mentioned that biochar can have the opposite effect in very basic soils, indicating that soil properties should be analyzed before applying the biochar. Xia et al (2023) also discuss how biochar provides a good microorganism habitat and therefore improves nitrogen fixation and nitrification. Figure 19 by Xia et al (2023) illustrates the nitrogen cycle within the soil.

The conclusion can also be drawn that process optimization will have minimal impact on the N-cycle, unless focused on increasing biochar yield, however, this inversely affects bio-oil yield. If external energy is needed it is important that it comes from renewable resources and not combustion of fossil fuels at high temperatures to avoid NOx gases being formed and affecting the N-cycle.

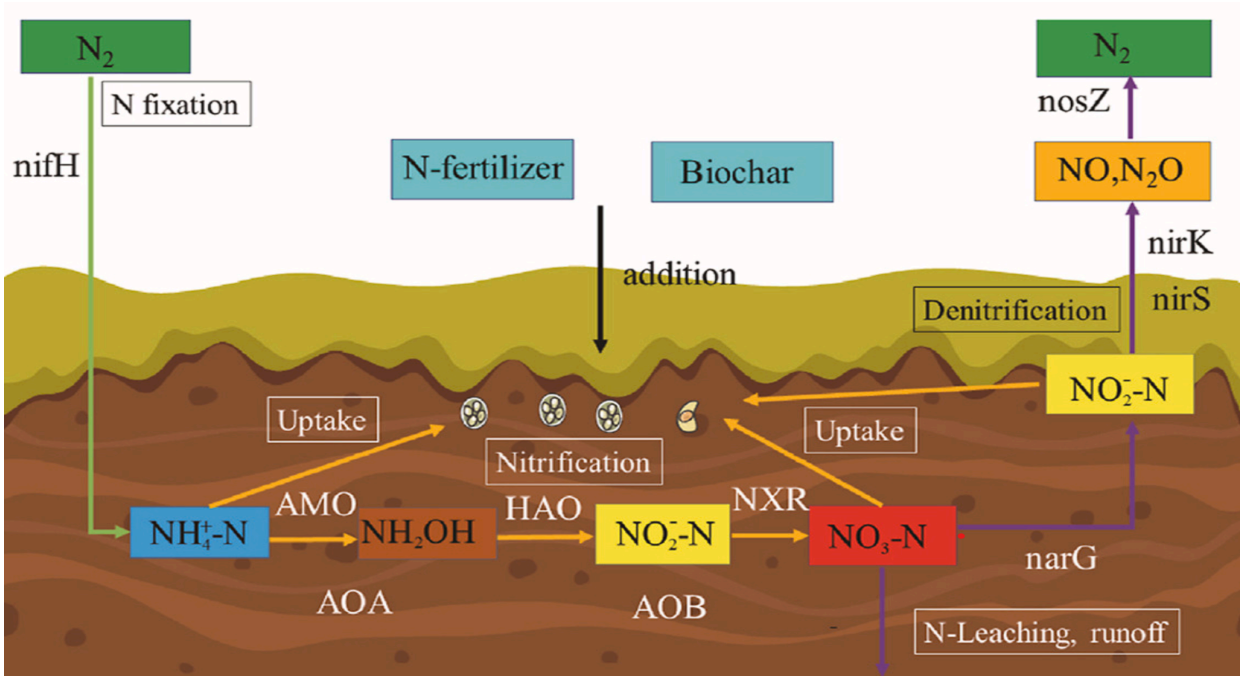

Figure 19: Figure by Xia et al (2023) showcasing nitrogen soil and bacteria interactions..

In summary, the main effect on the nitrogen cycle will come from the biochar, the increased N-fixation will impact the N-cycle by removing nitrogen from the atmosphere reducing the need of the added amount of nitrogen fertilizer to the ground. As well, the improved nitrification and nitrogen retention time will also affect the N-cycle by reducing the amount of nitrogen that will leave the soil back into the atmosphere through ammonia volatilisation. Biochar's ability to reduce N-leaching and run off will as well reduce the needed amount of applied fertilizer. Therefore, it is clear that using biochar will reduce the needed amount of added nitrogen fertilizer to the ground. This will in turn reduce the man-made impact on the natural N-cycle. Since less usage of nitrogen fertilizer will lead to reduced losses of NOx gases through denitrifying bacteria. Something that will improve both the environment and human health as described in the background. Using a lower amount of nitrogen fertilizer will also reduce runoff and N-leaching to the local ecosystem, reducing man-made eutrophication. Therefore, utilizing activated biochar with added nitrogen will reduce the man-made changes to the nitrogen cycle.

4.7 Sustainability Of The Process

For the biomass selection from a sustainable view, there is no point in selecting a biomass that needs to be transported far away for processing. Because the CO2 production from the transportation will at one point outway the benefits of the biomass processing. Therefore there will never be only one optimal feedstock for this specific process all around the world. The biomass has to be selected on the basis of close geographical accessibility and available amount. After these considerations it is important to look as mentioned in section 2.2 factors like social impact, biodiversity and also land use to prevent deforestation and competition with food production. A type of sustainable biomass that meets all of this criteria is crop residue, this includes husks, straw and stower. Another favorable source of biomass forest residue, such as sawdust, forest debris and small logging residue. The use of this type of lignocellulosic feedstock is also

preferable since its produced biochar is resistant to degradation, ensuring that the CO2 sequestered stays in the soil. Bachmann et al (2023) concludes that a feedstock from bio waste is a good sustainable solution for syngas production. Also as mentioned in the background using lignocellulosic based furniture could be an interesting option of recycling and meeting sustainability demand while even improving the nitrogen content of the biochar. Other than the feedstock it is important that all parts of the process like unit production and worker rights meet sustainability demands.

5. Conclusion

The conclusion of this thesis is that the proposed system will help sequester carbon up to 70% of the biomass carbon put into this process. However, as mentioned before the amount of actual sequestered carbon is dependent on the subsequent use of the syngas. Process optimization was also shown to be important to maximize the syngas yield and potential carbon sequestration of the process. A combined steam/CO2 reforming was seen to increase the yield of the wanted syngas products. The carbon sequestration potential of this process will help mitigate global warming, improve the environment and help the C-cycle to go back to a more natural state. It was also concluded that the heat produced in the Mild combustion will be enough for the whole process, however, this will need to be further investigated.

The usage of activated biochar, as a fertilizer, will help reduce the amount of nitrogen fertilizer needed to be applied to the soil. This is mainly due to the reduced ammonia volatilization and the higher retention of the nitrogen in the soil leading to higher plant uptake, this will help N-cycle to a more natural state. Additionally, it will improve the environment by decreasing the production of NOx gases from denitrifying bacteria and mitigating eutrophication caused by nitrogen fertilizer runoff from the soil.

6. Future work

There are a lot of available improvements to this process. Using more detailed reaction kinetics like in the work of Peters et al (2017) could improve the accuracy of the modeled pyrolysis. A more detailed study of the actual carbon sequestration possibility for the produced syngas depending on the finished products.

The actual heat transportation possibilities for the heat produced in the Mild combustion with added accounts for heat losses and heat transfer. Further validation on the Mild combustion and the CO2 reforming using rGibbs by experimental research.

Study the activation of the biochar even further, doing a better analysis on how different methods for combining the biochar with the nitrogen can lead to improvements in soil-N losses and a good nitrogen release ratio from the biochar.

7. Reference list

Bachmann, M., Völker, S., Kleinekorte, J. and Bardow, A. (2023). Syngas from What? Comparative Life-Cycle Assessment for Syngas Production from Biomass, CO_2, and Steel Mill Off-Gases. *ACS Sustainable Chemistry & Engineering*, 11(14), pp.5356–5366. doi:https://doi.org/10.1021/acssuschemeng.2c05390.

Bednik, M., Agnieszka Medyńska-Juraszek and Irmina Ćwieląg-Piasecka (2022). Effect of Six Different Feedstocks on Biochar's Properties and Expected Stability. *Agronomy*, 12(7), pp.1525–1525. doi:https://doi.org/10.3390/agronomy12071525.

Boylston, A. (2018). *How to ensure energy efficiency in mining 1/4: Comminution circuit design*. [online] Metso. Available at: https://www.metso.com/insights/blog/mining-and-metals/how-to-ensure-energy-efficiency-in-mining-part-one/ [Accessed 30 May 2024].

Brtnicky, M., Mustafa, A., Tereza Hammerschmiedt, Antonin Kintl, Lukas Trakal, Beesley, L., Ryant, P., Omara-Ojungu, C., Baltazar, T. and Jiri Holatko (2023). Pre-activated biochar by fertilizers mitigates nutrient leaching and stimulates soil microbial activity. *Chemical and biological technologies in agriculture*, 10(1). doi:https://doi.org/10.1186/s40538-023-00430-7.

Calonaci, M., Grana, R., Barker Hemings, E., Bozzano, G., Dente, M. and Ranzi, E. (2010). Comprehensive Kinetic Modeling Study of Bio-oil Formation from Fast Pyrolysis of Biomass. *Energy & Fuels*, [online] 24(10), pp.5727–5734. doi:https://doi.org/10.1021/ef1008902.

Caudle, B., Gorensek, M.B. and Chen, C.-C. (2019). A rigorous process modeling methodology for biomass fast pyrolysis with an entrained‐flow reactor. 2(1). doi:https://doi.org/10.1002/amp2.10031.

Cavaliere, A. and de Joannon, M. (2004). Mild Combustion. *Progress in Energy and Combustion Science*, 30(4), pp.329–366. doi:https://doi.org/10.1016/j.pecs.2004.02.003.

Chen, D., Cen, K., Zhuang, X., Gan, Z., Zhou, J., Zhang, Y. and Zhang, H. (2022). Insight into biomass pyrolysis mechanism based on cellulose, hemicellulose, and lignin: Evolution of volatiles and kinetics, elucidation of reaction pathways, and characterization of gas, biochar and bio‐oil. *Combustion and Flame*, 242, p.112142. doi:https://doi.org/10.1016/j.combustflame.2022.112142.

Cornelissen, G., Pandit, N.R., Taylor, P., Pandit, B.H., Sparrevik, M. and Schmidt, H.P. (2016). Emissions and Char Quality of Flame-Curtain 'Kon Tiki' Kilns for Farmer-Scale Charcoal/Biochar Production. *PLOS ONE*, [online] 11(5), p.e0154617. doi:https://doi.org/10.1371/journal.pone.0154617.

Debiagi, P.E.A., Pecchi, C., Gentile, G., Frassoldati, A., Cuoci, A., Faravelli, T. and Ranzi, E. (2015). Extractives Extend the Applicability of Multistep Kinetic Scheme of Biomass Pyrolysis. *Energy & Fuels*, [online] 29(10), pp.6544–6555. doi:https://doi.org/10.1021/acs.energyfuels.5b01753.

DeLacy, J. (2018). *NOx: A Refresher Course | 2018-01-11 | Engineered Systems Magazine*. [online] www.esmagazine.com. Available at: https://www.esmagazine.com/articles/98656-nox-a-refresher-course#:~:text=There%20are%20three%20types%20of [Accessed 29 May 2024].

Demiral, İ. and Şensöz, S. (2006). Fixed-Bed Pyrolysis of Hazelnut (Corylus AvellanaL.) Bagasse: Influence of Pyrolysis Parameters on Product Yields. *Energy Sources, Part A: Recovery, Utilization, and Environmental Effects*, 28(12), pp.1149–1158. doi:https://doi.org/10.1080/009083190966126.

Devi, P. and Saroha, A.K. (2014). Risk analysis of pyrolyzed biochar made from paper mill effluent treatment plant sludge for bioavailability and eco-toxicity of heavy metals. *Bioresource Technology*, 162, pp.308–315. doi:https://doi.org/10.1016/j.biortech.2014.03.093.

Encyclopedia Britannica (2018). Nitrogen Cycle | Definition & Steps. In: *Encyclopædia Britannica*. [online] Available at: https://www.britannica.com/science/nitrogen-cycle.

Franciski, M.A., Peres, E.C., Godinho, M., Perondi, D., Foletto, E.L., Collazzo, G.C. and Dotto, G.L. (2018). Development of CO2 activated biochar from solid wastes of a beer industry and its application for methylene blue adsorption. *Waste Management*, 78, pp.630–638. doi:https://doi.org/10.1016/j.wasman.2018.06.040.

Fu, M., Qi, W., Xu, Q., Zhang, S. and Yan, Y. (2016). Hydrogen production from bio-oil model compounds dry (CO2) reforming over Ni/Al2O3 catalyst. *International Journal of Hydrogen Energy*, 41(3), pp.1494–1501. doi:https://doi.org/10.1016/j.ijhydene.2015.11.104.

Gorensek, M.B., Shukre, R. and Chen, C.-C. (2019). Development of a Thermophysical Properties Model for Flowsheet Simulation of Biomass Pyrolysis Processes. *ACS Sustainable Chemistry & Engineering*, 7(9), pp.9017–9027. doi:https://doi.org/10.1021/acssuschemeng.9b01278.

Hama Aziz, K.H. and Kareem, R. (2023). Recent advances in water remediation from toxic heavy metals using biochar as a green and efficient adsorbent: A review. *Case Studies in Chemical and Environmental Engineering*, [online] 8, p.100495. doi:https://doi.org/10.1016/j.cscee.2023.100495.

Han, M., Zhang, J., Zhang, L. and Wang, Z. (2023). Effect of biochar addition on crop yield, water and nitrogen use efficiency: A meta-analysis. *Journal of Cleaner Production*, [online] 420, p.138425. doi:https://doi.org/10.1016/j.jclepro.2023.138425.

Humbird, D., Trendewicz, A., Braun, R. and Dutta, A. (2017). One-Dimensional Biomass Fast Pyrolysis Model with Reaction Kinetics Integrated in an Aspen Plus Biorefinery Process Model. *ACS Sustainable Chemistry & Engineering*, 5(3), pp.2463–2470. doi:https://doi.org/10.1021/acssuschemeng.6b02809.

IEA Bioenergy. (n.d.). *Pyrolysis Reactors*. [online] Available at: https://task34.ieabioenergy.com/pyrolysis-reactors/.

Jedynak, K. and Charmas, B. (2021). Preparation and Characterization of Physicochemical Properties of Spruce Cone Biochars Activated by CO2. *Materials*, [online] 14(14), p.3859. doi:https://doi.org/10.3390/ma14143859.

Jerzak, W., Reinmöller, M. and Magdziarz, A. (2022). Estimation of the heat required for intermediate pyrolysis of biomass. *Clean Technologies and Environmental Policy*, 24(10), pp.3061–3075. doi:https://doi.org/10.1007/s10098-022-02391-1.

Jindo, K., Audette, Y., Higashikawa, F.S., Silva, C.A., Akashi, K., Mastrolonardo, G., Sánchez-Monedero, M.A. and Mondini, C. (2020). Role of biochar in promoting circular economy in the agriculture sector. Part 1: A review of the biochar roles in soil N, P and K cycles. *Chemical and Biological Technologies in Agriculture*, 7(1). doi:https://doi.org/10.1186/s40538-020-00182-8.

Kaminsky, W. (2021). Chemical recycling of plastics by fluidized bed pyrolysis. *Fuel Communications*, 8, p.100023. doi:https://doi.org/10.1016/j.jfueco.2021.100023.

Kittelson, D., Watts, W., Bennett, D., Taff, S. and Chan, C. (n.d.). *Fuel of the Future - DME | Thomas E Murphy Engine Research Laboratory*. [online] merl.umn.edu. Available at: https://merl.umn.edu/cdr/dme.

Kumar, P. and Singh, S. (2016). *Valorizing Industrially Produced CO2: A reliable and cost effective solution for carbon capture and its conversion to marketable products*. [online] Available at:

https://eralberta.ca/wp-content/uploads/2017/05/K130099-Enerkem-Valorizing-CO2-Final-Report_PUBLIC.pdf.

Landa, L., Aingeru Remiro, José Valecillos, Bilbao, J. and Gayubo, A.G. (2023a). Thermodynamic study of the CO2 valorization in the combined steam-dry reforming of bio-oil into syngas. *Journal of CO2 utilization*, 72, pp.102503–102503. doi:https://doi.org/10.1016/j.jcou.2023.102503.

Landa, L., Remiro, A., Iglesias, S., Valecillos, J., Gayubo, A. and Bilbao, J. (2023b). Syngas Production through Dry Reforming of Raw Bio-oil: Effect of CO2/C Ratio. *Chemical Engineering Transactions*, [online] 99, pp.355–360. doi:https://doi.org/10.3303/CET2399060.

Landa, L., Remiro, A., Valecillos, J., Bilbao, J. and Gayubo, A.G. (2023c). Syngas production through combined steam-dry reforming of raw bio-oil over a NiAl2O4 spinel derived catalyst. *Journal of CO2 Utilization*, [online] 78, p.102637. doi:https://doi.org/10.1016/j.jcou.2023.102637.

Li, L., Rowbotham, J.S., Christopher Greenwell, H. and Dyer, P.W. (2013). *Chapter 8 - An Introduction to Pyrolysis and Catalytic Pyrolysis: Versatile Techniques for Biomass Conversion*. [online] ScienceDirect. Available at: https://www.sciencedirect.com/science/article/pii/B9780444538789000096.

Liu, X., Yang, S., Zang, C., Huang, H. and Varodi, A.M. (2023). *Comparative study on slow pyrolysis products of abandoned furniture materials :: BioResources*. [online] bioresources.cnr.ncsu.edu. Available at: https://bioresources.cnr.ncsu.edu/resources/comparative-study-on-slow-pyrolysis-products-of-abandoned-furniture-materials/.

Lou, H., Chen, D., Martin, C., Li, X., Li, K., Vaid, H., Singh, K.D. and Gangadharan, P. (2012). Optimal Reduction of the C1−C3 Combustion Mechanism for the Simulation of Flaring. *Industrial & Engineering Chemistry Research*, 51. doi:https://doi.org/10.1021/ie2027684.

Lyu, G., Wu, S. and Zhang, H. (2015). Estimation and Comparison of Bio-Oil Components from Different Pyrolysis Conditions. *Frontiers in Energy Research*, 3. doi:https://doi.org/10.3389/fenrg.2015.00028.

Pahnila, M., Koskela, A., Petri Sulasalmi and Timo Fabritius (2023). A Review of Pyrolysis Technologies and the Effect of Process Parameters on Biocarbon Properties. *Energies*, 16(19), pp.6936–6936. doi:https://doi.org/10.3390/en16196936.

Peters, J.F., Banks, S.W., Bridgwater, A.V. and Dufour, J. (2017). A kinetic reaction model for biomass pyrolysis processes in Aspen Plus. *Applied Energy*, [online] 188, pp.595–603. doi:https://doi.org/10.1016/j.apenergy.2016.12.030.

Ranzi, E., Debiagi, P.E.A. and Frassoldati, A. (2017). Mathematical Modeling of Fast Biomass Pyrolysis and Bio-Oil Formation. Note I: Kinetic Mechanism of Biomass Pyrolysis. *ACS Sustainable Chemistry & Engineering*, 5(4), pp.2867–2881. doi:https://doi.org/10.1021/acssuschemeng.6b03096.

Riebeek, H. (2011). *The Carbon Cycle*. [online] NASA. Available at: https://earthobservatory.nasa.gov/features/CarbonCycle.

Sies, M.M. and Mazlan Abdul Wahid (2020). Numerical Investigation of the Asymmetrical Vortex Combustor Running on Biogas. *Journal of Advanced Research in Fluid Mechanics and Thermal Sciences*, 74(1), pp.1–18. doi:https://doi.org/10.37934/arfmts.74.1.118.

US Department of Commerce, N.O. and A.A. (2022). *What is the carbon cycle?* [online] oceanservice.noaa.gov. Available at: https://oceanservice.noaa.gov/facts/carbon-cycle.html#:~:text=The%20carbon%20cycle%20is%20nature.

utslappisiffror.naturvardsverket.se. (n.d.). *Nitrogen oxides (NOx)*. [online] Available at: https://utslappisiffror.naturvardsverket.se/en/Substances/Other-gases/Nitrogen-oxides/.

Wiebren De Jong and Ommen, V. (2015). *Biomass as a sustainable energy source for the future : fundamentals of conversion processes*. Hoboken, N.J.: Wiley.

Xia, H., Riaz, M., Tang, X., Yan, L., Zeinab El-Desouki, Li, Y., Wang, X. and Jiang Cuncang (2023). Insight into mechanisms of biochar-fertilizer induced of microbial community and microbiology of nitrogen cycle in acidic soil. *Journal of environmental management*, 336, pp.117602–117602. doi:https://doi.org/10.1016/j.jenvman.2023.117602.

Xiong, J., Zhang, S., Ke, L., Wu, Q., Zhang, Q., Cui, X., Dai, A., Xu, C., Cobb, K., Liu, Y., Ruan, R. and Wang, Y. (2023). Research progress on pyrolysis of nitrogen-containing biomass for fuels, materials, and chemicals production. *Science of the total environment*, 872, pp.162214–162214. doi:https://doi.org/10.1016/j.scitotenv.2023.162214.

Appendix A

Appendix A gives the chosen temperature and splitfraction for the different configurations, as well as for calculated CO2/C ratio, the specific H2 and CO concentrations, and CO2 conversion.
[Appendix A.pdf]

Appendix B

Carbon and energy Sankey diagram for configuration 2.

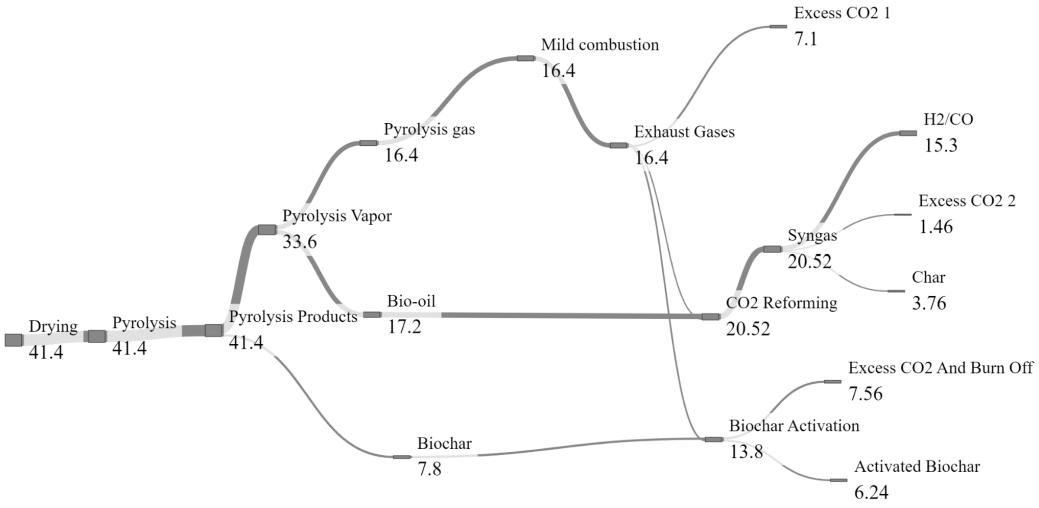

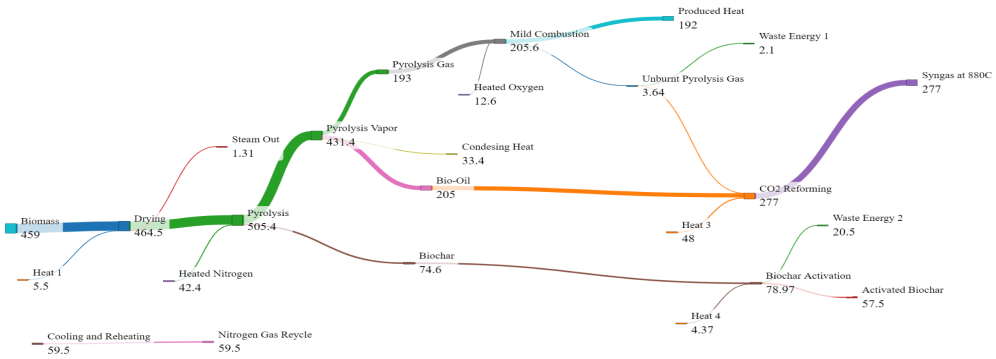

Appendix C

Appendix C includes the amount of energy generated in the Qstoic for the different compounds, and the subsequently calculated LHV-values.

Configuration 1	Q (J/s)	Q (MJ/hr)	Mass KG/hr	Water Mass Out	LHV MJ/KG
Bio-oil	226293	814.6548	42	27.9	17.88079042
Pyrolysis gas	170688	614.4768	31.4	17.05	18.24333439
Biochar	72612	261.4032	8.54	0.8689	30.36081337
Biomass	458856	1651.8816	83.4	47.52	18.41532086
Syngas	255639	920.3004	66.1	28.2	12.88102874
Configuration 2	Q (J/s)	Q (MJ/hr)	Mass KG/hr	Water Mass Out	LHV MJ/KG
Bio-oil	204793	737.2548	38	24.8	17.80771579
Pyrolysis gas	192756	693.9216	35.2	20.22	18.31091932
Biochar	71931	258.9516	8.45	0.81	30.41107456
Biomass	458856	1651.8816	83.4	47.52	18.41532086
Syngas	234512	844.2432	50.3	25.08	15.56655746
Configuration 3	Q (J/s)	Q (MJ/hr)	Mass KG/hr	Water Mass Out	LHV MJ/KG
Bio-oil	226293	814.6548	42	27.9	17.88079042
Pyrolysis gas	170688	614.4768	31.4	17.05	18.24333439
Biochar	72612	261.4032	8.54	0.8689	30.36081337
Biomass	458856	1651.8816	83.4	47.52	18.41532086
Syngas	265776	956.7936	69.3	31.3	12.70359307
Optimization	Q (J/s)	Q (MJ/hr)	Mass KG/hr	Water Mass Out	LHV MJ/KG
Bio-oil	262621	945.4356	47	31.7	18.64145961
Pyrolysis gas	137838	496.2168	28.16555611	13.66	16.43351469
Biochar	69269	249.3684	7.970269316	0.4594127906	31.14656533
Biomass	458856	1651.8816	83.4	47.52	18.41532086
Syngas	293381	1056.1716	70.7	31.8	13.84039604